Journal Pre-proof

Discovery of heterocycle-containing α-naphthoflavone derivatives as water-soluble, highly potent and selective CYP1B1 inhibitors

Jinyun Dong, Guang Huang, Qing Cui, Qingqing Meng, Shaoshun Li, Jiahua Cui

PII: S0223-5234(20)30867-9

DOI: https://doi.org/10.1016/j.ejmech.2020.112895

Reference: EJMECH 112895

To appear in: *European Journal of Medicinal Chemistry*

Received Date: 2 June 2020

Revised Date: 2 September 2020

Accepted Date: 24 September 2020

Please cite this article as: J. Dong, G. Huang, Q. Cui, Q. Meng, S. Li, J. Cui,, Discovery of heterocycle-containing α-naphthoflavone derivatives as water-soluble, highly potent and selective CYP1B1 inhibitors, *European Journal of Medicinal Chemistry*, https://doi.org/10.1016/j.ejmech.2020.112895.

Graphical abstract:

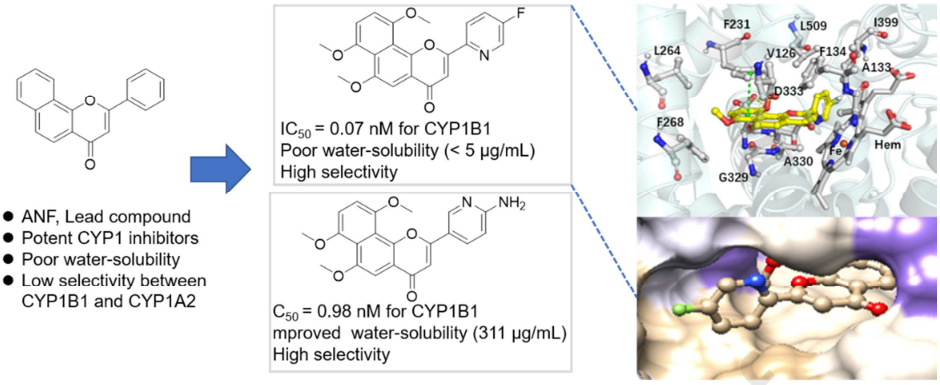

Discovery of heterocycle-containing α-naphthoflavone derivatives as water-soluble, highly potent and selective CYP1B1 inhibitors

Jinyun Dong[1,2], Guang Huang[1], Qing Cui[1], Qingqing Meng[1], Shaoshun Li[1]* and Jiahua Cui[1, 3]**

[1] School of Pharmacy, Shanghai Jiao Tong University, 800 Dongchuan Road, Shanghai, China

[2] College of Pharmaceutical Sciences, Zhejiang Chinese Medical University, Hangzhou, China

[3] School of Environmental Science and Engineering, Shanghai Jiao Tong University, 800 Dongchuan Road, Shanghai, China

*Corresponding Author; **Corresponding Author.

E-mail addresses: cpucjh@sjtu.edu.cn (J. Cui), ssli@sjtu.edu.cn (S. Li).

Abstract

Cytochrome P450 1B1 (CYP1B1) has been well validated as an attractive target for cancer prevention and drug resistance reversal. In continuation of our interest in this area, herein, a set of forty-six 6,7,10-trimethoxy-α-naphthoflavone derivatives varying in B ring was synthesized and screened against CYP1 enzymes, leading to the identification of fluorine-containing compound **15i** as the most potent and selective CYP1B1 inhibitor (IC_{50} value of 0.07 nM), which was 84-fold more potent than that of the template molecule ANF. In addition, the amino-substituted derivative **13h** not only possessed a potent inhibitory effect on CYP1B1 (IC_{50} value of 0.98 nM), but also had a substantially increased water solubility as compared with the lead ANF (311 μg/mL for **13h** and < 5 μg/mL for ANF). The current study expanded the structural diversity of CYP1B1 inhibitors, and compound **13h** could be considered as a promising starting point with great potential for further studies.

Keywords: CYP1 enzymes, CYP1B1 inhibitors, α-naphthoflavone derivatives, SARs.

1. Introduction

Cytochrome P450 enzymes (CYPs) belong to a superfamily of heme-dependent monooxygenases that are involved in the metabolic biotransformation of a wide variety of structurally diverse endogenic and xenobiotic chemicals, including many approved drugs [1]. Among them, the cytochrome P450 subfamily 1 enzymes (CYP1s) including CYP1A1, CYP1A2, and CYP1B1 have long been of interest for their dominant roles in the bioactivation of numerous procarcinogens—compounds (such as polycyclic aromatic hydrocarbons) to mutagenic and carcinogenic derivatives [2]. They are expressed in a tissue-specific manner: CYP1A2 is located primarily in the liver, while CYP1A1 and CYP1B1 are mainly expressed in extrahepatic tissues

such as breast, prostate and endometrium [3, 4]. Various planar aromatic molecules including 7,12- dimethylbenz[a]anthracene (DMBA) and 2,3,7,8-tetrachlorodibenzo-*p*-dioxin (TCDD) could stimulate the expression levels of CYP1s by binding to the aryl hydrocarbon receptor (AhR), a ligand-activated transcription factor [5-7].

CYP1B1 isoform is the most attractive therapeutic target among the three CYP1 members mentioned above for the following reasons: (1) CYP1B1 is constitutively overexpressed to a notable extent in tumors (breast, testis, colon, lung, *etc*.), although the expression levels of these enzymes differ between tumor and corresponding normal tissues [8], (2) besides its role in the bioactivation of many exogenous procarcinogens, CYP1B1 catalyzes the 4-hydroxylation of endogenic 17β-estradiol (E_2) leading to the formation of E_2-3,4-quinone, a mutagenic compound able to bind DNA covalently, thereby contributing to estrogen carcinogenesis, and (3) it confers drug resistance by metabolically inactivating structurally diverse anticancer drugs such as docetaxel, mitoxantrone, doxorubicin and paclitaxel [9]. Therefore, strategy that contributes to the selective inhibition of CYP1B1 could be therapeutically beneficial for preventing mammary tumor formation and countering CYP1B1-associated drug resistance [9].

Over the past years, various kinds of compounds including flavonoids, *trans*-stilbenes, coumarins, phytoestrogens and alkaloids have been characterized as CYP1 inhibitors [4, 10, 11]. Among them, flavonoids have been extensively studied since they have diverse medicinal applications and are less likely to induce toxicity [12, 13]. α-Naphthoflavone (ANF), a synthetic flavonoid, has long been determined as one of the most potent CYP1 inhibitors. Shimada et al. found ANF could considerably inhibit the recombinant human CYP1B1, CYP1A2 and CYP1A1 with IC_{50} values of 5, 6 and 60 nM, respectively [14]. As a consequence, ANF not only functions as a chemopreventive agent, but also as a chemosensitizing agent to reverse the CYP1B1-mediated drug resistance [15]. Similar to the most flavonoids, ANF possesses a broad safety profile [16]. All these promising properties of ANF make it a potential candidate for further study. Nevertheless, poor water solubility and low selectivity toward CYP1B1 over the other CYP1 isoforms (especially CYP1A2 isoform) remain the limitations to its applications as both chemical tools and therapeutics [17].

To this end, our research group recently has made great efforts toward the development of potent and selective CYP1B1 inhibitors with improved water solubility by structural modification of ANF (shown in Fig.1), however, such a compound has not yet been discovered [11, 17-19]. We introduced three methoxy groups to the naphthalene moiety of ANF and found that their CYP1 inhibition ability obviously enhanced compared with ANF [17]. Notably, compound **4c** (structure shown in Fig.1) exhibited strong CYP1B1 inhibitory activity with an IC_{50} value as low as 0.043

nM. Regrettably, its water solubility is much lower for successful use in cell-based study. Structural modification of the C ring of ANF including introduction of functional groups to the C3 position, reduction of the C2-C3 double bond, or isosteric replacement of oxygen atom at 1-position with “NH” or “S” led to varying degrees of loss of CYP1 inhibition, indicating C ring is indispensable for maintaining the blocking activity. [18, 19]. However, incorporation of substituents into the B ring pronouncedly affects their inhibitory capacity and selectivity toward CYP1B1 [17, 18]. In addition, aromatic heterocycles are tolerated for potency in CYP1 inhibition [18]. Based on these findings, herein we describe our efforts to identify and characterize novel aromatic heterocycle substituted α-naphthoflavone derivatives as water-soluble, potent and selective CYP1B1 inhibitors.

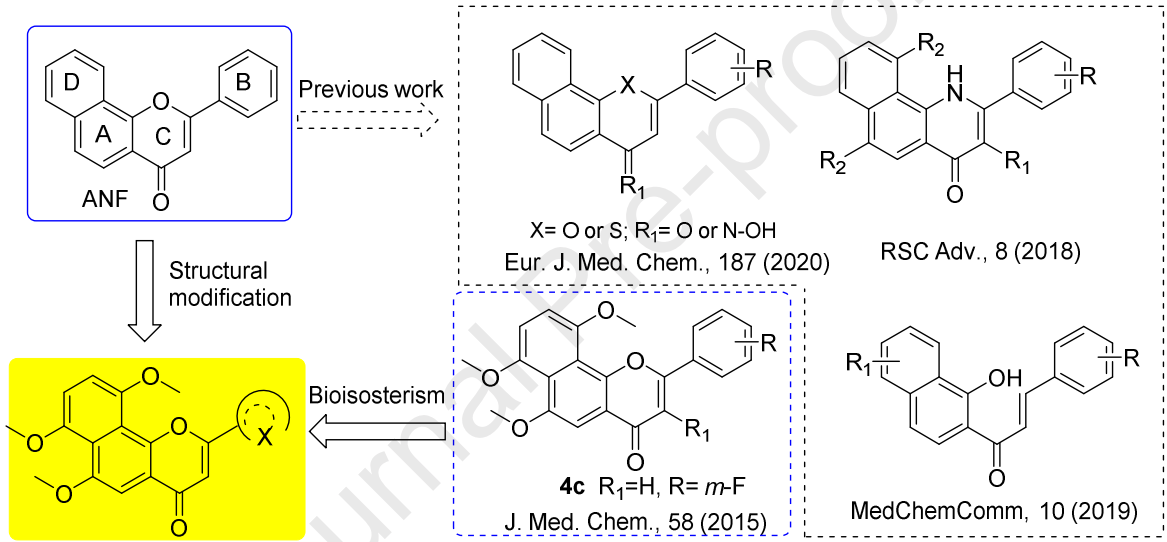

Fig 1. Summary of our previous and current work.

2. Results and discussion

2.1. Chemistry

All the compounds studied were synthesized according to the procedures described in Scheme 1 (the synthetic routes for preparation of some aromatic acid intermediates were not shown here). Methylation of commercially available 1,5-dihydroxynaphthalene (**1**) followed by bromination and methoxylation provided 1,4,5,8-tetramethoxynaphthalene (**4**). Vilsmeier reaction of **4** with *N*,*N*-dimethylformamide and phosphorus oxychloride gave 2-formyl-1,4,5,8-tetramethoxynaphthalene (**5**), which was reacted with Grignard reagent (CH_3MgI) to give the alcohol **6**. Oxidation of **6** with active manganese dioxide afforded the corresponding ketone derivative **7**, which was subjected to selective demethylation in the presence of aluminum chloride to yield the key intermediate **8**. The ester derivatives **9**, obtained by the esterification reaction of **8** with various aromatic acids in the presence of EDCI (or HATU)

and DMAP at room temperature, were treated with NaH to undergo Baker-Venkataraman rearrangement to furnish the corresponding 1,3-dione derivatives **10**. Acid-catalyzed cyclization reaction of **10** provided the final compounds in good yields.

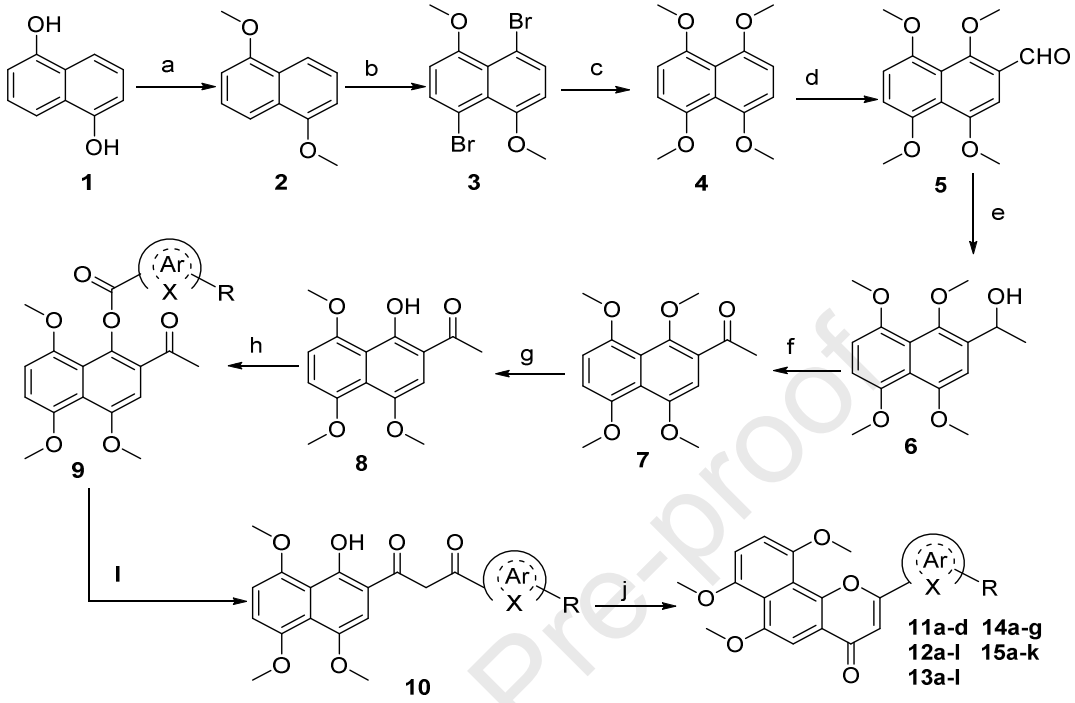

Scheme 1. Reagents and conditions: (a) KOH, $(CH_3)_2SO_4$, rt.; (b) CH_3CN, NBS, -10 ^oC; (c) CH_3ONa, CuI, reflux; (d) $POCl_3$, DMF, reflux; (e) CH_3MgI, Et_2O, NH_4Cl, rt.; (f) MnO_2, DCM, reflux; (g) $AlCl_3$, CH_3CN, 60 ^oC; (h) EDCI/DMAP or HATU/DMAP; (i) NaH, DMF; (j) 10% H_2SO_4-EtOH, reflux.

2.2. CYP1 enzyme inhibitory activities

The inhibitory effects of these studied compounds on recombinant human CYP1 enzymes were measured by the EROD (7-ethoxyresorufin O-deethylation) assay as described previously [17]. In our previous study, we found that introduction of a piperazine moiety to the B ring of ANF resulted in a slight decrease of CYP1B1 inhibitory activity, while morpholine ring was shown to be tolerated (two- and single-digit nanomolar IC_{50} values, respectively). In light of the importance of nitrogen-containing heterocycles in improving water solubility, hence, at the start of this study, we attempted to introduce three methoxy groups into the naphthalene moiety of ANF, aiming to increase their CYP1B1 inhibitory potency. The results are presented in Table 1. Out of our expectation, all of these piperazine-substituted derivatives (compounds **11a-b** and **11d**) suffered a great loss of inhibitory effects on CYP1 enzymes (IC_{50} values of > 500 nM). Consistently, morpholine-substituted derivative (**11c**) was the most potent one among them, however, compared with ANF or the previously reported compound that does not contain three methoxy groups, analog **11c** still showed a somewhat loss of activity in blocking CYP1B1

enzyme (IC_{50} values of 5.9, 2 and 14.9 nM, respectively) [18]. From these results we speculate that the introduction of multi-methoxy groups would lead to unfavorable conformations of these aliphatic heterocycles within the active sites.

Table 1. Inhibitory activities of 6,7,10-trimethoxy-α-naphthoflavone derivatives against CYP1s

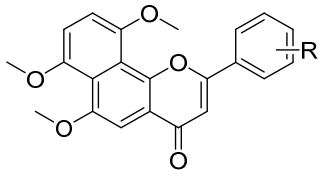

Compd.	R	IC_{50} values (nM)			IC_{50} ratio	
		1B1	1A1	1A2	1A1/1B1	1A2/1B1
11a	3-(4-methyl-piperazin-1-yl)	>1000	>1000	>1000	-	-
11b	3-Cl-5-(4-methyl-piperazin-1-yl)	519.4	>1000	>1000	>1.9	>1.9
11c	3-(4-morpholinyl)	14.9	132.5	>1000	8.9	>67.1
11d	4-(4-methyl-piperazin-1-yl)	>1000	>1000	>1000	-	-
ANF	-	5.9	80.3	18.0	13.6	3.1

Considering that aliphatic heterocycles may not be suitable for ANF-based skeleton, we turned our attention to replacing the phenyl ring with various aromatic heterocycles. Herein, we synthesized a variety of aromatic heterocycle ring-substituted α-naphthoflavone derivatives to determine an optimal one. In this part, an initial set of heteroaromatic fused-ring derivatives including **12a-h** was designed and synthesized to evaluate whether a bigger substituent could enhance the CYP1B1 inhibitory activity. As shown in Table 2, all of these analogs, except **12f**, exhibited potent inhibition of CYP1B1 with IC_{50} values ranging from 0.87 to 15.6 nM, while showing weak or no inhibitory effect toward CYP1A2 with IC_{50} values more than 1000 nM. Compound **12a** incorporating an indole ring was found to potently inhibit CYP1B1 with an IC_{50} value of 0.95 nM. Based on this compound, we observed that: (1) reversal of the indole ring resulted in 4-fold decrease in CYP1B1 inhibitory potency (compound **12g**, IC_{50} = 4.1 nM), whereas bioisosteric replacement of the nitrogen atom of **12g** with an oxygen atom afforded compound **12h** with a comparable activity with **12a** (IC_{50} = 0.87 nM); (2) addition of a nitrogen atom to the indole ring yielding compounds **12b-c** and **12f** caused a differential decrease in inhibitory activity toward CYP1B1, especially compound **12f**, which showed more than100-fold

loss in potency against CYP1B1, however, out of our expectation, it was able to selectively inhibit CYP1A1(IC_{50} values of 189.4 and 23.8 nM for CYP1B1 and CYP1A2, respectively); (3) addition of a carbon atom to the pyrrole ring of indole providing the corresponding quinoline derivative **12d** that showed only a minimal loss of CYP1B1 inhibitory activity with an IC_{50} value of 1.8 nM and, interestingly, the activity was increased when its quinoline functionality was reversed (compound **12e**, IC_{50} = 1.0 nM). Taking these observations together, we could postulate that CYP1B1 and CYP1A1 inhibitory efficacies are affected by the position and number of nitrogen atom on the B ring, but, of note, the nitrogen atom is not an essential structural element for these compounds.

Some single-ring substituted derivatives including **12i-l** and **13a-15a** were also synthesized and evaluated to explore the structure-activity relationship (SAR) in this series. As presented in Table 2, all of these five- and six-membered ring substituted derivatives had a potent inhibitory effect on CYP1B1 with IC_{50} values ranging from sub-nanomole to nanomole levels. However, compared with the fused-ring derivatives above, all of these single-ring derivatives, except **12l**, showed a significant increase in activity against CYP1A2, suggesting that CYP1A2 may be more sensitive to steric hindrance than that of the other two isozymes. Removal of the phenyl moiety of compound **12h** led to furan derivative **12i**, which showed a comparable potency against CYP1B1 (IC_{50} = 1.2 nM). However, replacement of the oxygen atom of compound **12i** with a sulfur atom was unfavorable for CYP1B1 inhibition (**12j**, IC_{50} = 4.8 nM), but it was able to be partially restored by introducing a nitrogen atom (**12k**, IC_{50} = 2.6 nM), suggesting the importance of physicochemical properties of aromatic heterocycles such as electron cloud density and lipophilicity. To improve water solubility, we further explored four nitrogen-containing six-membered ring derivatives **12l** and **13a-15a**. Three pyridine substituted analogs **13a-15a** showed similar CYP1B1 inhibitory activities with IC_{50} values around 1 nM, which was more potent than pyridazine derivative **12l** (IC_{50} = 2.0 nM). In light of their CYP1B1 inhibitory potency, selectivity and water-soluble potential, our attention was drawn to the development of pyridine substituted derivatives as CYP1B1 inhibitors.

Table 2. Inhibitory activities of heterocyclic ring-substituted 6,7,10-trimethoxy-α-naphthoflavone derivatives toward CYP1 enzymes

171

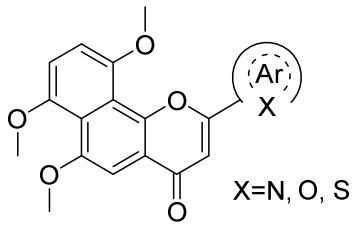

Compd.	Ar	IC_{50} values (nM)			IC_{50} ratio	
		1B1	1A1	1A2	1A1/1B1	1A2/1B1
12a	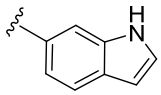	0.95	141.9	>1000	149.4	>1052.6
12b	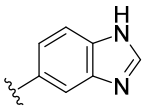	15.6	42.4	>1000	2.7	>64.1
12c	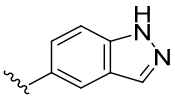	2.0	1.6	>1000	0.8	>500
12d	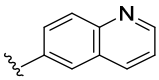	1.8	20.9	>1000	11.6	>555.6
12e	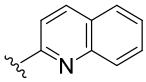	1.0	117.6	>1000	117.6	>1000
12f	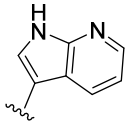	189.4	23.8	>1000	0.1	>5.3
12g	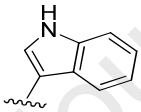	4.1	16.5	>1000	4.0	>243.9
12h	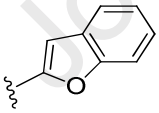	0.87	10.1	>1000	11.6	>1149.4
12i	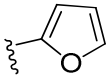	1.2	13.8	67.2	11.5	56.0
12j	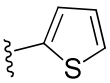	4.8	4.4	40.4	0.9	8.4
12k	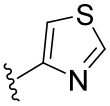	2.6	3.1	29.2	1.2	11.2
12l	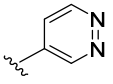	2.0	125.7	>1000	62.9	>500
13a	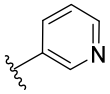	1.0	7.6	117.3	7.6	117.3

Compd.	Ar	IC_{50} values (nM)			IC_{50} ratio	
		1B1	1A1	1A2	1A1/1B1	1A2/1B1
14a	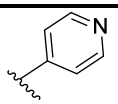	1.2	40.4	199.8	33.7	166.5
15a	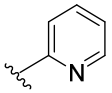	0.6	5.4	107.6	9.0	179.3
ANF	-	5.9	80.3	18.0	13.6	3.1

A series of pyridin-3-yl substituted α-naphthoflavone derivatives was first synthesized and their biological data were shown in Table 3. In our previous studies, the meta-position of B ring in α-naphthoflavone scaffold was found to be very critical for CYP1B1 inhibitory potency. Therefore, we initially focused our efforts on introducing several substituents into the meta-position (C-5') of pyridin-3-yl ring. Compounds **13b-d** bearing halogen or methyl group showed a noticeable potency in blocking CYP1B1 with a very high selectivity profile over CYP1A2, being five-fold more potent than ANF (their IC_{50} values around 1 nM). By contrast, analogs **13e-g** attaching hydrophilic functionalities such as amino, carboxyl and hydroxy showed a drop in CYP1B1 inhibitory activity, with IC_{50} values at tens of nanomolar concentrations. To improve their activity against CYP1B1, we moved these hydrophilic substituents to the C-4' or C-2' positions. To our delight, compound **13h**, whose structure was characterized by an amino substituent at C-4' position, considerably increased the inhibitory effect on CYP1B1 with an IC_{50} value of 0.98 nM. Furthermore, it maintained high selectivity over the other two isozymes. Surprisingly, a dramatic drop in enzymatic activity was observed when the amino was replaced by a hydroxy (**13i**, IC_{50} = 658.3 nM), or was moved to C-2' position (**13k**, IC_{50} = 175.2 nM). Of note, substitutions on the C-2' position (**13j-l**) were less active than the corresponding C-5' or C-4' substituted derivatives in blocking CYP1B1, suggesting that substitution at the 2'-position was detrimental to the activity.

Table 3. Inhibitory activities of pyridin-3-yl substituted 6,7,10-trimethoxy-α-naphthoflavone derivatives toward CYP1s

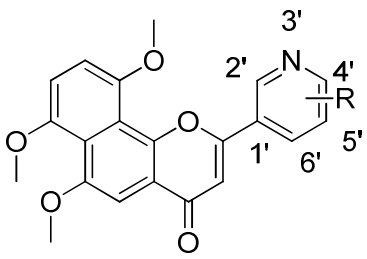

Compd.	R	IC_{50} values (nM)			IC_{50} ratio	
		1B1	1A1	1A2	1A1/1B1	1A2/1B1
13a	H	1.0	7.6	117.3	7.6	117.3
13b	5'-F	0.98	17.7	140.6	18.1	143.5
13c	5'-Br	1.1	8.0	742.0	7.3	674.5
13d	5'-CH_3	1.3	6.9	160.7	5.3	123.6
13e	5'-NH_2	22.9	18.8	628.5	0.8	27.4
13f	5'-COOH	30.1	85.8	>1000	2.9	>33.2
13g	5'-OH	10.3	80.9	>1000	7.9	>97.1
13h	4'-NH_2	0.98	30.8	108.0	31.4	110.2
13i	4'-OH	658.3	>1000	>1000	>1.5	>1.5
13j	2'-OH	>1000	151.9	>1000	0.2	-
13k	2'-NH_2	175.2	137.1	>1000	0.8	>5.7
13l	2'-Br	63.9	60.7	965.5	0.9	15.1
ANF	-	5.9	80.3	18.0	13.6	3.1

Next, a set of pyridin-4-yl substituted α-naphthoflavone derivatives was carried out to confirm the effect of the type of pyridine ring on CYP1 enzymes. Similarly, we also focused our optimization efforts on the meta-position (3'-position) of B ring in α-naphthoflavone scaffold and the results are summarized in Table 4. Compared with ANF, halogen group substituted analogs **14b-d** were more potent and selective in blocking CYP1B1 enzyme (IC_{50} values ranging from 0.46 to 1.1 nM), while hydroxy- and amino-substituted derivatives **14e** and **14f** were significantly less potent (IC_{50} values of 61.5 and 20.6, respectively). Analog **14g**, obtained by removing the amino to the 2'-position, showed a slight loss of CYP1B1 inhibitory activity compared to **14f**, which confirmed our hypothesis of the importance of structural modification at 3'-position. Among them, compound **14d** attaching a bromine atom at 3'-position was characterized as the most potent and selective CYP1B1 inhibitor, with an IC_{50} value of 0.46 nM. Consistent with the SAR observed in Table 3, hydrophobic-substituted derivatives were generally more potent than the corresponding hydrophilic ones. It is interesting to note that a significant reduction in CYP1A2 inhibitory efficacy was observed as compared with **14a** and the other compounds presented in Table 4, indicating that larger substituents in the B ring would not be accommodated by the active site of CYP1A2.

Table 4. Inhibitory activities of pyridin-4-yl substituted 6,7,10-trimethoxy-α-naphthoflavone derivatives toward CYP1s

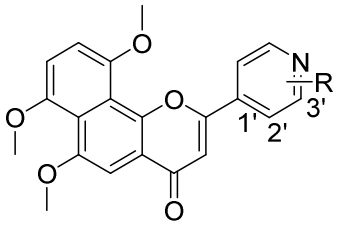

Compd.	R	IC_{50} values (nM)			IC_{50} ratio	
		1B1	1A1	1A2	1A1/1B1	1A2/1B1
14a	H	1.2	40.4	199.8	33.7	166.5
14b	3'-F	0.93	38.9	518.0	41.8	557.0
14c	3'-Cl	1.1	91.6	>1000	83.3	>909.1
14d	3'-Br	0.46	26.9	>1000	58.5	>2173.9
14e	3'-OH	61.5	232.0	>1000	3.8	>16.3
14f	3'-NH_2	20.6	15.3	>1000	0.7	>48.5
14g	2'-NH_2	24.8	31.6	>1000	1.3	>40.3
ANF	-	5.9	80.3	18.0	13.6	3.1

With the goal of gaining more potent CYP1B1 inhibitors and exploring SAR, we finally turned our attention to expanding a series of pyridin-2-yl substituted α-naphthoflavone derivatives as CYP1B1 inhibitors. Several meta-position (3'-position) substituted derivatives including **15b-f** were synthesized and enzyme inhibition data are given in Table 5. Consistent with the above results, hydrophobic functionality-containing analogs **15d-f** were more active than the hydrophilic-substituted derivatives **15b** and **15c** in suppressing CYP1 enzymes. Particularly, halogen-substituted compounds **15e** and **15f** were found to have outstanding ability to inhibit CYP1B1 with IC_{50} values of 0.38 and 0.3 nM, respectively. To determine whether CYP1B1 inhibitory ability could be improved by modification at the other positions of pyridin-2-yl ring, we synthesized another two compounds **15g** and **15h** with chlorine atom incorporated at the 4'- and 5'-position, respectively. To our surprise, compound **15g** was found to be more potent than **15h** and **15f** in inhibiting CYP1B1 enzyme with an IC_{50} value of 0.14 nM, indicating the importance of 4'-position in CYP1 enzymes. Keeping this in mind, an attempt has been made to find out more potent CYP1B1 inhibitors by introducing fluorine and bromine atoms at 4'-position

of the pyridin-2-yl ring. Gratifyingly, fluorine-substituted derivative **15i** showed two-fold more potent CYP1B1 inhibitory activity than **15g** with an IC_{50} value as low as 0.07 nM, being the most potent CYP1B1 inhibitor. Analysis of the data presented in Tables 3-5, we can easily conclude that amino-substituted derivatives generally displayed higher CYP1B1 inhibitory activity than the corresponding hydroxyl-substituted compounds. In light of the critical roles of amino group in improving water solubility and further chemical modification, herein, we continued to introduce an amino group to the 4'-position. However, the resulting compound **15k** still remained a comparable level of CYP1B1 inhibitory activity to that of ANF.

Table 5. Inhibitory activities of pyridin-2-yl substituted 6,7,10-trimethoxy-α-naphthoflavone derivatives toward CYP1s

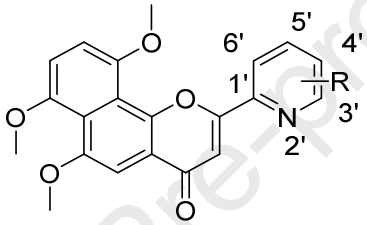

Compd.	R	IC_{50} values (nM)			IC_{50} ratio	
		1B1	1A1	1A2	1A1/1B1	1A2/1B1
ANF	-	5.9	80.3	18.0	13.6	3.1
15a	H	0.6	5.4	107.6	9.0	179.3
15b	3'-NH_2	6.5	56.8	>1000	8.7	>153.8
15c	3'-OH	7.7	322.6	>1000	41.9	>129.9
15d	3'-CH_3	1.2	19.9	148.2	16.6	123.5
15e	3'-F	0.38	2.3	668.4	6.1	1758.9
15f	3'-Cl	0.30	5.7	348.6	19.0	1162
15g	4'-Cl	0.14	1.6	208.5	11.4	1489.3
15h	5'-Cl	0.84	9.9	>1000	11.8	>1190.5
15i	4'-F	0.07	16.8	>1000	240	>14285.7
15j	4'-Br	1.3	38.9	622.8	29.9	479.1
15k	4'-NH_2	6.0	66.6	>1000	11.1	>166.7

3. Molecular docking studies

In an attempt to gain insight into the probable binding modes and rationalize the observed

CYP1B1 inhibitory efficacy and selectivity of the most potent compound **15i**, molecular docking studies have been carried out using GOLD 5.3.0 software (Cambridge, UK). The crystal structures of ANF in complex with CYP1B1 (PDB ID: 3PM0) and CYP1A2 (PDB ID: 2HI4) were used for this study. As shown in parts A to C in Fig. 2, compound **15i** snugly fits well into the active site of CYP1B1 and it is involved in hydrophobic contacts with residues F231, L264, F268, G329, A330, A133, I399, F134, V126 as well as L509. An enhanced π-π stacking interaction between the naphthalene part and phenyl ring of F231 caused by increased electron density of the naphthalene part provides a strong binding affinity. Also, the methoxy group forms a hydrogen bond with D333 with a distance of 2.6 Å. The docked complex was structurally superimposed on the ligand ANF (Fig 2B), and it showed that the pyridine moiety of compound **15i** is closer to heme than that of ANF (distances of 3.0 and 4.3 Å, respectively), which is unfavorable for formation of the reactive heme iron-oxo intermediate during catalysis. The surface map of docked complex indicated that the pyridine moiety of compound **15i** is surrounded by a hydrophobic region (colored by brown), which is favorable for hydrophobic contact with fluorine substituent. Further, it also provides an explanation for the fact that compounds incorporating a hydrophobic substituent on the pyridine ring generally showed better CYP1B1 inhibitory effects than those with hydrophilic substituents. As can be seen from parts D and E in Fig. 2, compound **15i** docked in the active site of CYP1A2 with a similar pose to that in CYP1B1. It binds to a hydrophobic pocket formed by amino acid residues F226, L497, I386, T124, A317, G316 and F260, with the pyridine moiety being closer to heme than that of ANF. However, it does not form a hydrogen bond (or water-mediated hydrogen bond[20]) with any residues as compared with ANF (ANF forms a water-mediated hydrogen bond with Gly316), which may provide a partial explanation for a lower activity of compound **15i** against CYP1A2.

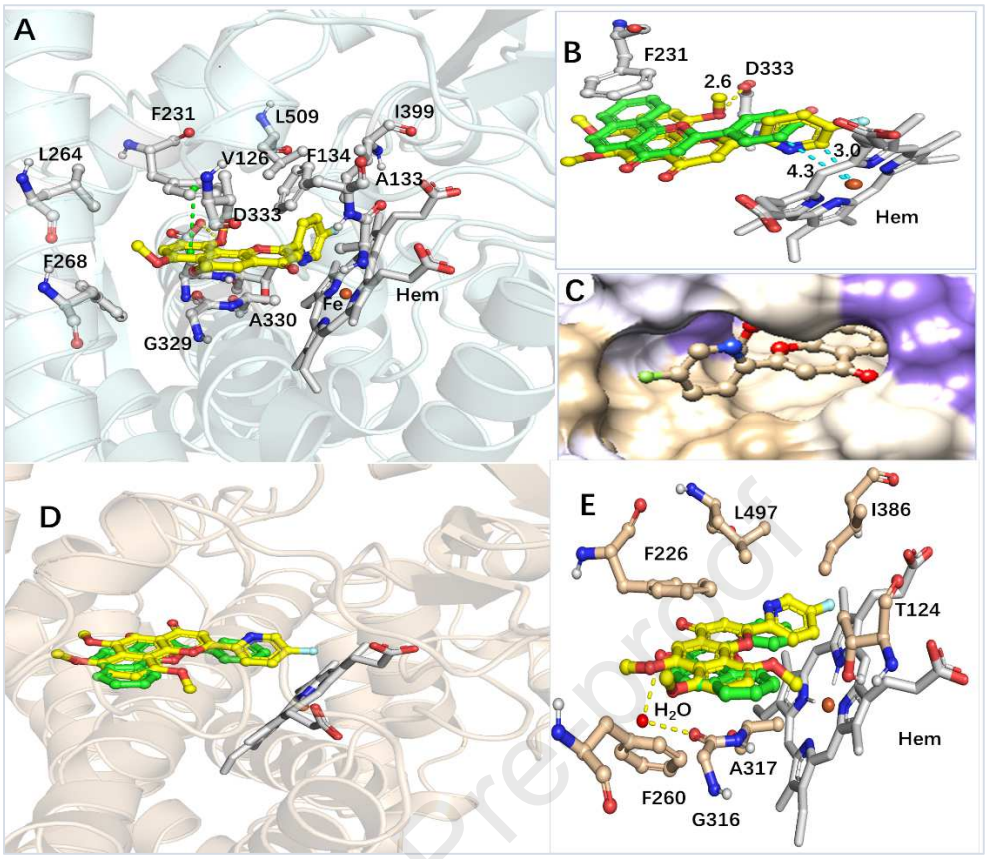

Fig 2. Molecular docking study of compound **15i** in CYP1B1(A-C) and CYP1A2 (D-E) (compound **15i**: yellow stick; ANF: green stick; yellow dash line: hydrogen bond; green dash line: π-π stacking interaction; cyan dash line: distance)

Considering that the total score (expressed as -log(K_d), including crash score and polar score) generated by Surflex-Dock may directly predict the binding affinity of the ligand-protein complex, therefore we calculated their parameters using another molecular docking software SYBYL-X 2.0 (Tripos Inc., St. Louis, USA) to confirm the observed biological results again. Compound **15i** and the template molecule ANF were docked into the active sites of CYP1B1 and CYP1A2 and the highest scores are presented in Table 6. Surprisingly, a high correlation was found between the total scores and the activities (-logIC_{50}). The total score of compound **15i** in CYP1B1 was much higher than that in CYP1A2 with values of 8.5969 and 4.1880, respectively, while ANF possessed similar total scores in CYP1B1 and CYP1A2 with values of 6.9669 and 7.1981, respectively. Furthermore, compound **15i** showed a higher total score than ANF in CYP1B1 with values of 8.5969 and 6.9669, respectively, whereas it displayed a lower total score than ANF in CYP1B1 with values of 4.1880 and 7.1981, respectively. These results are consistent with experimentally observed trends in CYP1 inhibitory potency. It should be noted that compound **15i** reached a very low crash score of -7.4502, indicating a high degree of inappropriate penetration by this compound into the binding site of CYP1A2. Based on the previous finding that the volume of the CYP1A2 cavity is smaller than that of CYP1B1 (size

values of 375 and 398 $Å^3$, respectively) [21], therefore, it might be speculated that steric hindrance is another critical factor for contributing to the lower CYP1A2 inhibitory efficacy of compound **15i**.

Table 6. Surflex-Dock scores of compound **15i** and ANF

Compd.	IC_{50} values (nM)		Docking score in CYP1B1			Docking score in CYP1A2		
	CYP1B1	CYP1A2	Total Score	Crash Score	Polar Score	Total Score	Crash Score	Polar Score
15i	0.07	>1000	8.5969	-2.5712	0.0001	4.1880	-7.4502	1.1228
ANF	5.9	18.0	6.9699	-0.3755	0.0000	7.1981	-0.3857	0.1418

(Total score, expressed as -log(K_d), represent binding affinities; Crash score, degree of inappropriate penetration by the ligand into the protein and interpenetration between ligand atoms that are separated by rotatable bonds of compounds. c) Polar score, the contribution of polar non-hydrogen bonding interactions to the total score)

4. Determination of water solubility

A suitable water solubility of a compound (drug) is one of the most important properties for obtaining reliable *in vitro* and *in vivo* assay results in early drug discovery and for ensuring sufficient concentration in circulation to get a desired therapeutic exposure [22]. ANF is a potent CYP1 inhibitor, but it has poor water solubility that may limit its efficacy and further development [17]. In this study, some of these synthesized α-naphthoflavone derivatives have been selected to determine whether their water solubility was improved. Compound **15i** as the most potent and selective CYP1B1 inhibitor among them was first selected to evaluate its water solubility by a standard HPLC method. Unfortunately, similar to ANF, the saturated solution concentration of compound **15i** in water was undetectable, indicating poor water solubility (presented in Table 7). As a result, we transformed the compound **15i** to its hydrochloride and sulfate forms. Regrettably, an enhanced water solubility still cannot be achieved, for its salt forms were unstable in water and they could restore to the prototype form immediately.

In light of the fact that the amino-substituted α-naphthoflavone derivatives are more potent than the corresponding hydroxyl-substituted derivatives in blocking CYP1B1, and simultaneously they are more alkaline and less hydrophobic (lower ClogP, calculated by Chembiodraw Ultra 14.0) than compound **15i**, in spite of a slight loss of CYP1B1 inhibitory, we turned our attention to the compound **13h**, the most potent CYP1B1 inhibitor among the amino-substituted series. To our surprise, compound **13h** showed more than 60-fold of improvement in water solubility as compared with ANF and compound **15i** (311 μg/mL for **13h**,

< 5 μg/mL for ANF and **15i**). It is interesting to note that a remarkably increased water solubility was also observed for its salt form, for example, the water solubility of its sulfate form was up to 4910 μg/mL. it suggested that compound **13h** may be a promising starting point with great potential for further studies.

Table 7. Water solubility of the selected compounds.

Compd.	ClogP	Water solubility (μg/mL)	
		Free base	Salt form
ANF	4.65	< 5	/
15i	3.75	< 5	< 5
13h	2.99	311	4910

4. Conclusion

In this study, structural modification of ANF gave a series of forty-six 6,7,10-trimethoxy-α-naphthoflavone derivatives, which exhibited varying levels of inhibitory potency on CYP1 enzymes. SAR analysis indicated that the CYP1 inhibitory efficacy was greatly determined by the type and position of the substituents on the B ring. Among them, the fluorine-containing derivative **15i** showed excellent selectivity for CYP1B1 over the other two CYP1 isoforms and was characterized as the most potent inhibitor for CYP1B1 with an IC_{50} value of 0.07 nM, with 84-fold more potent inhibition than ANF as the lead compound. Molecular modeling study revealed that appropriate binding site conformation, hydrophobic interactions and an enhanced π-π stacking interactions were the predominant factors contributing to its high CYP1B1 inhibitory activity. Additionally, the amino-substituted derivative **13h** not only possessed a potent inhibitory effect on CYP1B1, but also had a substantially increased water solubility as compared with ANF as determined by solubility assay, suggesting that it may have a great potential for further study. The follow-up study of reversal of drug resistance by compound **13h** *in vitro* and *in vivo* is currently underway and will be reported upon completion.

5. Experimental section

5.1. Chemistry

All starting materials and reagents were either obtained from commercial suppliers or prepared according to literature reported procedures. All solvents were used as supplied without further purification unless otherwise indicated. Anhydrous solvents were dried according to standard methods. Proton nuclear magnetic resonance (^{1}H NMR) and ^{13}C NMR spectra were

recorded with Varian Mercury-300 (400 MHz) spectrometer. Chemical shifts (δ scale) are reported in parts per million (ppm) downfield from tetramethylsilane (TMS) and coupling constants (*J*) are expressed in hertz (Hz). Multiplicities are shown as the following abbreviations: s (singlet), brs (broad singlet), d (doublet), t (triplet), m (multiplet). Reactions were monitored by thin-layer chromatography (TLC, silica gel GF_{254}) and visualized with UV light (254 or 365 nm). Column chromatography was conducted on silica gel (200-300 mesh). High resolution mass spectrometry (HRMS) were obtained on Agilent 6540 QTOF (ESI).

5.2. General procedure for preparation of all the α-naphthoflavone derivatives

The intermediates **2-8** were easily prepared from 1,5-dihydroxynaphthalene (**1**) according to our previously reported procedures[23]. To a stirred solution of 1-(1-hydroxy-4,5,8-trimethoxynaphthalen-2-yl)ethan-1-one (**8,** 2 mmol) in dry DMF (10 mL), commercially available or laboratory prepared aromatic benzoic acid derivative (2.2 mmol), condensing agent EDCI/DMAP (3 mmol/3mmol) or HATU/DMAP were added. The resultant solution was stirred at ambient temperature for overnight when TLC showed that the reaction was complete. The reaction mixture was poured into an ice-water solution and extracted with EtOAc. The combined organic layers were washed with saturated NaCl aqueous, and dried over Na_2SO_4. The solvent was removed under reduced pressure and the crude residue was subjected to silica gel column chromatography to give intermediate **9**.

NaH was added to a mixture of intermediate **9** (1 mmol) in dry DMF (5 mL) under N_2 and The mixture was stirred at ambient temperature for 5 h. After being quenched with acetic acid ice-water solution and the precipitate obtained was filtered. After drying, the red crude product **10** can be used directly without further purification.

Intermediate **10** (0.5 mmol) was suspended to H_2SO_4-EtOH solution (10%, 25 mL) and the resultant mixture was kept for stirring at temperature of 90 °C till the completion of the reaction as indicated by TLC. After removing solvents under vacuum, the residue was dissolved in water, neutralized by $NaHCO_3$ and extracted with EtOAc. The organic layers were washed with saturated brine, dried over anhydrous Na_2SO_4, and concentrated under reduced pressure. The residue was purified by column chromatography using silica gel to give all the studied compounds in this work.

5.2.2. 6,7,10-trimethoxy-2-(3-(4-methylpiperazin-1-yl)phenyl)-4*H*-benzo[*h*]benzopyran-4-one (**11a**)

Yellow solid; yield 69%; ^{1}H NMR (400 MHz, $CDCl_3$) δ 7.63 – 7.55 (m, 2H), 7.46 (d, *J* = 6.5 Hz, 1H), 7.36 (t, *J* = 8.0 Hz, 1H), 7.07 (d, *J* = 8.8 Hz, 1H), 7.02 (d, *J* = 5.7 Hz, 2H), 6.91 (s,1H), 4.01

(s, 6H), 3.88 (s, 3H), 3.29 – 3.24 (m, 4H), 2.61 – 2.56 (m, 4H), 2.33 (s, 3H). ^{13}C NMR (101 MHz, $CDCl_3$) δ 177.73, 163.59, 154.39, 151.88, 151.75, 151.39, 149.17, 133.25, 129.62, 122.35, 121.51, 118.68, 117.78, 114.11, 113.13, 109.70, 109.56, 107.28, 98.95, 58.20, 57.03, 56.61, 54.98, 49.03, 46.03. HRMS (ESI) calcd for $[C_{27}H_{28}N_2O_5 + H]^+$ 461.2076, found 461.20977.

5.2.2. 2-(3-chloro-5-(4-methylpiperazin-1-yl)phenyl)-6,7,10-trimethoxy-4*H*-benzo[*h*]benzopyran -4-one (**11b**).

Yellow solid; yield 62%; ^{1}H NMR (400 MHz, $CDCl_3$) δ 7.58 (s, 1H), 7.31 (s, 1H), 7.18 (s, 1H), 6.95 (d, *J* = 8.8 Hz, 1H), 6.91 – 6.84 (m, 2H), 6.79 (s, 1H), 3.96 (s, 3H), 3.93 (s, 3H), 3.81 (s, 3H), 3.24 – 3.16 (m, 4H), 2.54 – 2.50 (m, 4H), 2.30 (s, 3H). ^{13}C NMR (101 MHz, $CDCl_3$) δ 177.39, 161.62, 154.38, 152.30, 151.46, 151.02, 148.85, 135.61, 134.04, 122.09, 121.31, 118.03, 117.89, 117.38, 112.87, 111.05, 108.72, 106.97, 98.53, 57.91, 56.43, 56.28, 54.76, 48.50, 46.04. HRMS (ESI) calcd for $[C_{27}H_{27}ClN_2O_5 + H]^+$ 495.1687, found 495.17089.

5.2.3. 6,7,10-trimethoxy-2-(3-morpholinophenyl)-4*H*-benzo[*h*]benzopyran-4-one (**11c**).

Yellow solid; yield yield73%; ^{1}H NMR (400 MHz, $CDCl_3$) δ 7.72 – 7.61 (m, 2H), 7.50 (s, 1H), 7.44 (t, *J* = 7.8 Hz, 1H), 7.17 – 7.02 (m, 3H), 6.96 (s, 1H), 4.06 (s, 3H), 4.04 (s, 3H), 3.93 (s, 3H), 3.93 – 3.86 (m, 4H), 3.31 – 3.22 (brs, 4H). ^{13}C NMR (101 MHz, $CDCl_3$) δ 177.66, 163.33, 154.43, 151.76, 151.54, 151.39, 149.12, 133.34, 129.73, 122.28, 121.48, 118.63, 118.59, 118.40, 113.89, 112.99, 109.75, 107.28, 98.84, 66.76, 58.15, 57.01, 56.58, 49.54. HRMS (ESI) calcd for $[C_{26}H_{25}NO_6 + H]^+$ 448.1760, found 448.17656.

5.2.4. 6,7,10-trimethoxy-2-(4-(4-methylpiperazin-1-yl)phenyl)-4*H*-benzo[*h*]benzopyran-4-one (**11d**).

Yellow solid; yield 65%; ^{1}H NMR (400 MHz, $CDCl_3$) δ 7.84 (d, *J* = 8.6 Hz, 2H), 7.39 (s, 1H), 6.93 (d, *J* = 8.8 Hz, 1H), 6.85 (d, *J* = 9.0 Hz, 3H), 6.72 (s, 1H), 3.95 (s, 3H), 3.91 (s, 3H), 3.81 (s, 3H), 3.35 – 3.22 (m, 4H), 2.54 – 2.45 (m, 4H), 2.28 (s, 3H). ^{13}C NMR (101 MHz, $CDCl_3$) δ 177.43, 163.30, 154.03, 152.88, 151.51, 151.06, 148.79, 127.56, 121.99, 121.76, 121.24, 118.31, 114.40, 112.49, 108.70, 104.70, 99.00, 57.93, 56.49, 56.44, 54.71, 47.53, 46.07. HRMS (ESI) calcd for $[C_{27}H_{28}N_2O_5 + H]^+$ 461.2076, found 461.20804.

5.2.5 2-(1*H*-Indol-6-yl)-6,7,10-trimethoxy-4*H*-benzo[*h*]benzopyran-4-one (**12a**)

Brown solid; yield 74%; ^{1}H NMR (400 MHz, DMSO-d_6) δ 11.63 (s, 1H), 8.36 (s, 1H), 7.82 (dd, *J* = 8.5, 1.4 Hz, 1H), 7.73 – 7.65 (m, 1H), 7.62 – 7.51 (m, 1H), 7.36 – 7.29 (m, 2H), 7.28 – 7.23 (m,

1H), 7.12 (s, 1H), 6.53 (s, 1H), 4.17 (s, 3H), 3.92 (s, 3H), 3.83 (s, 3H). ^{13}C NMR (101 MHz, DMSO-d_6) δ 176.30 , 164.42 , 154.45 , 151.30 , 151.22 , 148.54, 136.17 , 130.76 , 129.27 , 124.48 , 121.56 , 121.22 , 120.99 , 118.04 , 117.50 , 113.46 , 110.48 , 110.40 , 105.74 , 102.16 , 98.63 , 57.89 , 57.41 , 56.60 . HRMS (ESI) calcd for $[C_{24}H_{19}NO_5 + H]^+$ 402.1341, found 402.13443.

5.2.6. 2-(1*H*-benzo[*d*]imidazol-5-yl)-6,7,10-trimethoxy-4*H*-benzo[*h*]benzopyran-4-one (**12b**)

Brown solid; yield 68%; ^{1}H NMR (400 MHz, DMSO-d_6) δ 13.14 – 12.69 (m, 1H), 8.67 (brs, 1H), 8.42 (brs, 1H), 8.11 (brs, 1H), 7.79 (brs, 1H), 7.38 – 7.27 (m, 3H), 7.24 (s, 1H), 4.19 (s, 3H), 3.96 (s, 3H), 3.86 (s, 3H). HRMS (ESI) calcd for $[C_{23}H_{18}N_2O_5 + H]^+$ 403.1294, found 403.12986.

5.2.7. 2-(1*H*-indazol-5-yl)-6,7,10-trimethoxy-4*H*-benzo[*h*]benzopyran-4-one (**12c**)

Brown solid; yield 45%; ^{1}H NMR (400 MHz, DMSO-d_6) δ 13.34 (s, 1H), 8.66 (s, 1H), 8.26 (s, 1H), 8.10 (d, J = 8.7 Hz, 1H), 7.68 (d, J = 8.7 Hz, 1H), 7.30 – 7.15 (m, 3H), 7.09 (s, 1H), 4.08 (s, 3H), 3.88 (s, 3H), 3.79 (s, 3H). HRMS (ESI) calcd for $[C_{23}H_{18}N_2O_5 + H]^+$ 403.1294, found 403.12917.

5.2.8. 6,7,10-Trimethoxy-2-(quinolin-6-yl)-4*H*-benzo[*h*]benzopyran-4-one (**12d**)

Brown solid; yield 72%; ^{1}H NMR (400 MHz, $CDCl_3$) δ 8.95 (d, J = 4.0 Hz, 1H), 8.50 (s, 1H), 8.24 – 8.10 (m, 3H), 7.44 (dd, J = 8.2, 4.2 Hz, 1H), 7.40 (s, 1H), 7.10 – 7.04 (m, 1H), 7.03 – 6.95 (m, 2H), 4.08 (s, 3H), 4.00 (s, 3H), 3.90 (s, 3H). ^{13}C NMR (101 MHz, $CDCl_3$) δ 177.37, 161.69, 154.48, 151.81, 151.43, 151.26, 149.12, 149.00, 136.75, 130.09, 130.07, 127.83, 126.51, 126.17, 122.25, 121.98, 121.44, 118.19, 112.99, 109.02, 107.52, 98.69, 58.00, 56.53, 56.46. HRMS (ESI) calcd for $[C_{25}H_{19}NO_5 + H]^+$ 414.1341, found 414.13359.

5.2.9. 6,7,10-Trimethoxy-2-(quinolin-2-yl)-4*H*-benzo[*h*]benzopyran-4-one (**12e**)

Brown solid; yield 69%; ^{1}H NMR (400 MHz, DMSO-d_6) δ 8.74 (s, 1H), 8.51 (s, 1H), 8.11 (d, J = 24.7 Hz, 2H), 7.89 (s, 1H), 7.73 (s, 1H), 7.52 (s, 1H), 7.42-7.26 (m, 3H), 4.17 (s, 3H), 3.96 (s, 3H), 3.86 (s, 3H). ^{13}C NMR (101 MHz, pyridine) δ 176.87, 161.37, 155.11, 151.63, 151.59, 149.88, 149.61, 149.35, 148.87, 148.00, 137.35, 130.42, 130.07, 128.92, 127.99, 127.92, 122.59, 118.42, 113.40, 109.62, 108.53, 99.12, 57.64, 56.48, 56.07. HRMS (ESI) calcd for $[C_{25}H_{19}NO_5 + H]^+$ 414.1341, found 414.13420.

5.2.10. 6,7,10-Trimethoxy-2-(1*H*-pyrrolo[2,3-b] pyridin-3-yl)-4*H*-benzo[*h*]benzopyran-4-one

(**12f**)

Brown solid; yield 52%; ^{1}H NMR (400 MHz, DMSO-d_6) δ 12.55 (s, 1H), 8.57 (d, 1H), 8.41 – 8.37 (m, 2H), 7.37 (s, 1H), 7.34 – 7.30 (m, 1H), 7.30 – 7.25 (m, 2H), 6.92 (s, 1H), 4.05 (s, 3H), 3.95 (s, 3H), 3.86 (s, 3H). HRMS (ESI) calcd for $[C_{23}H_{18}N_2O_5 + H]^+$ 403.1294, found 403.12922.

5.2.11. 2-(1*H*-Indol-3-yl)-6,7,10-trimethoxy-4*H*-benzo[*h*]benzopyran-4-one (**12g**)

Brown solid; yield 68%; ^{1}H NMR (400 MHz, DMSO-d_6) δ 12.00 (s, 1H), 8.22 (s, 1H), 8.04 (d, *J* = 7.3 Hz, 1H), 7.55 (d, *J* = 7.3 Hz, 1H), 7.30 (s, 1H), 7.26 – 7.20 (m, 2H), 7.16 (s, 2H), 6.79 (s, 1H), 3.99 (s, 3H), 3.89 (s, 3H), 3.79 (s, 3H). ^{13}C NMR (101 MHz, DMSO-d_6) δ 175.80, 161.41, 154.07, 151.21, 151.10, 148.22, 137.53, 129.61, 123.87, 122.99, 121.70, 121.40, 120.91, 120.32, 117.84, 113.13, 112.92, 109.94, 108.75, 104.98, 98.80, 57.73, 56.98, 56.49. HRMS (ESI) calcd for $[C_{24}H_{19}NO_5 + H]^+$ 402.1341, found 402.13442.

5.2.12. 2-(benzofuran-2-yl)-6,7,10-trimethoxy-4*H*-benzo[*h*]benzopyran-4-one (**12h**)

Yellow solid; yield 59%; ^{1}H NMR (400 MHz, DMSO-d_6) δ 7.92 (d, *J* = 7.5 Hz, 1H), 7.80 – 7.66 (m, 2H), 7.51 (t, *J* = 7.5 Hz, 1H), 7.39 (t, *J* = 7.2 Hz, 1H), 7.30 (s, 3H), 6.91 (s, 1H), 4.16 (s, 3H), 3.94 (s, 3H), 3.85 (s, 3H). ^{13}C NMR (101 MHz, $CDCl_3$) δ 176.74, 155.68, 154.56, 154.55, 151.79, 151.27, 148.83, 148.46, 127.81, 126.69, 123.71, 122.26, 122.06, 121.57, 118.06, 113.21, 111.78, 109.37, 108.62, 106.68, 98.74, 58.05, 56.87, 56.52. HRMS (ESI) calcd for $[C_{24}H_{18}O_6 + H]^+$ 403.1182, found 403.11872.

5.2.13. 2-(furan-2-yl)-6,7,10-trimethoxy-4H-benzo[*h*]benzopyran-4-one (**12i**)

Yellow solid; yield 61%; ^{1}H NMR (400 MHz, DMSO-d_6) δ 8.00 (s, 1H), 7.18 (d, *J* = 3.3 Hz, 1H), 7.16 (s, 1H), 7.14 – 7.09 (m, 2H), 6.78 (dd, *J* = 3.2, 1.6 Hz, 1H), 6.59 (s, 1H), 3.96 (s, 3H), 3.86 (s, 3H), 3.78 (s, 3H). ^{13}C NMR (101 MHz, DMSO-d_6) δ 175.53, 154.48, 154.31, 151.21, 150.99, 147.91, 147.17, 146.44, 121.39, 121.17, 117.53, 113.62, 113.40, 113.28, 110.13, 104.41, 98.26, 57.68, 56.96, 56.43. HRMS (ESI) calcd for $[C_{20}H_{16}O_6 + H]^+$ 353.1025, found 353.10283.

5.2.14. 6,7,10-Trimethoxy-2-(thien-2-yl)-4*H*-benzo[*h*]benzopyran-4-one (**12j**)

Yellow solid; yield 63%; ^{1}H NMR (400 MHz, DMSO-d_6) δ 8.00 (d, *J* = 3.7 Hz, 1H), 7.93 (dd, *J* = 4.9, 0.9 Hz, 1H), 7.27 (dd, *J* = 4.9, 3.8 Hz, 1H), 7.24 (s, 1H), 7.21 – 7.16 (m, 2H), 7.00 (s, 1H), 4.04 (s, 3H), 3.89 (s, 3H), 3.79 (s, 3H). ^{13}C NMR (101 MHz, DMSO-d_6) δ 175.79, 158.58, 154.56, 151.30, 150.95, 148.10, 135.29, 132.09, 129.38, 129.17, 121.46, 121.20, 117.55, 113.46, 109.88, 105.31, 98.43, 57.79, 56.80, 56.50. HRMS (ESI) calcd for $[C_{20}H_{16}O_5S + H]^+$ 369.0797, found

369.08019.

5.2.15. 6,7,10-Trimethoxy-2-(thiazol-4-yl)-4*H*-benzo[*h*]benzopyran-4-one (**12k**)

Brown solid; yield 49%; ^{1}H NMR (400 MHz, DMSO-d_6) δ 9.33 (s, 1H), 8.33 (s, 1H), 7.31 – 7.19 (m, 3H), 7.00 (s, 1H), 4.10 (s, 3H), 3.92 (s, 3H), 3.83 (s, 3H). ^{13}C NMR (101 MHz, DMSO-d_6) δ 176.17, 158.07, 157.45, 154.65, 151.35, 151.11, 148.50, 148.32, 122.44, 121.53, 121.39, 117.67, 113.59, 110.33, 107.17, 98.36, 57.81, 57.28, 56.57; HRMS (ESI) calcd for $[C_{19}H_{15}NO_5S + H]^+$ 370.0749, found 370.07509.

5.2.16. 6,7,10-Trimethoxy-2-(pyridazin-4-yl)-4*H*-benzo[*h*]benzopyran-4-one (**12l**)

Brown solid; yield 41%; ^{1}H NMR (400 MHz, DMSO-d_6) δ 9.94 (s, 1H), 9.55 (d, J = 6.1 Hz, 1H), 8.32 (s, 1H), 7.57 (s, 1H), 7.35 – 7.19 (m, 3H), 4.09 (s, 3H), 3.91 (s, 3H), 3.81 (s, 3H). HRMS (ESI) calcd for $[C_{20}H_{16}N_2O_5 + H]^+$ 365.1137, found 365.11316.

5.2.17. 6,7,10-Trimethoxy-2-(pyridin-3-yl)-4*H*-benzo[*h*]benzopyran-4-one (**13a**)

Brown solid; yield 59%; ^{1}H NMR (400 MHz, DMSO-d_6) δ 9.45 (s, 1H), 8.79 (s, 1H), 8.61 (d, 1H), 7.74 – 7.66 (m, 1H), 7.41 – 7.26 (m, 4H), 4.10 (s, 3H), 3.96 (s, 3H), 3.86 (s, 3H). ^{13}C NMR (101 MHz, $CDCl_3$) δ 177.01, 160.14, 154.59, 151.69, 151.46, 151.16, 148.94, 147.66, 133.18, 128.12, 123.45, 122.23, 121.45, 118.03, 113.09, 108.84, 107.47, 98.58, 57.96, 56.45, 56.42. HRMS (ESI) calcd for $[C_{21}H_{17}NO_5 + H]^+$ 364.1185, found 364.11871.

5.2.18. 6,7,10-Trimethoxy-2-(pyridin-4-yl)-4*H*-benzo[*h*]benzopyran-4-one (**14a**)

Brown solid; yield 52%; ^{1}H NMR (400 MHz, DMSO-d_6) δ 8.87 (d, J = 5.7 Hz, 2H), 8.16 (d, J = 5.6 Hz, 1H), 7.43 (s, 1H), 7.35 – 7.23 (m, 1H), 4.12 (d, J = 2.7 Hz, 1H), 3.94 (s, 1H), 3.85 (s, 1H). ^{13}C NMR (101 MHz, $CDCl_3$) δ 177.22, 159.81, 154.83, 151.57, 151.32, 150.62, 149.09, 139.65, 122.40, 121.76, 119.71, 118.17, 113.35, 109.24, 108.57, 98.54, 58.08, 56.60, 56.55. HRMS (ESI) calcd for $[C_{21}H_{17}NO_5 + H]^+$ 364.1185, found 364.11881.

5.2.19. 6,7,10-Trimethoxy-2-(pyridin-2-yl)-4*H*-benzo[*h*]benzopyran-4-one (**15a**)

Brown solid; yield 62%; ^{1}H NMR (400 MHz, DMSO-d_6) δ 8.80 (d, J = 3.6 Hz, 1H), 8.40 (d, J = 7.7 Hz, 1H), 8.22 (t, J = 7.6 Hz, 1H), 7.69 – 7.61 (m, 1H), 7.36 – 7.14 (m, 4H), 4.14 (s, 3H), 3.95 (s, 3H), 3.86 (s, 3H). ^{13}C NMR (101 MHz, $CDCl_3$) δ 177.60, 161.10, 154.37, 151.34, 151.12, 149.94, 149.68, 148.63, 136.66, 125.07, 122.09, 121.88, 121.01, 118.04, 112.83, 108.86, 107.97, 98.78, 57.91, 56.44, 56.42. HRMS (ESI) calcd for $[C_{21}H_{17}NO_5 + H]^+$ 364.1185, found 364.11897.

5.2.20. 2-(5-fluoropyridin-3-yl)-6,7,10-trimethoxy-4*H*-benzo[*h*]benzopyran-4-one (**13b**)

Yellow solid; yield 67%; ^{1}H NMR (400 MHz, DMSO-d_6) δ 9.26 (s, 1H), 8.77 (d, J = 2.7 Hz, 1H), 8.41 (d, J = 9.7 Hz, 1H), 7.38 (s, 1H), 7.29 – 7.21 (m, 3H), 4.02 (s, 3H), 3.90 (s, 3H), 3.81 (s, 3H). ^{13}C NMR (101 MHz, $CDCl_3$) δ 176.95, 160.77, 158.57, 158.20, 154.84, 151.45, 151.29, 148.99, 143.10, 140.16, 139.92, 129.90, 122.36, 121.62, 120.37, 120.16, 113.28, 108.98, 108.16, 98.57, 58.05, 56.56, 56.42. HRMS (ESI) calcd for $[C_{21}H_{16}FNO_5 + H]^+$ 382.1091, found 382.10865.

5.2.21. 2-(5-Bromopyridin-3-yl)-6,7,10-trimethoxy-4*H*-benzo[*h*]benzopyran-4-one (**13c**)

Yellow solid; yield 64%; ^{1}H NMR (400 MHz, DMSO-d_6) δ 9.36 (s, 1H), 8.89 (s, 1H), 8.80 (s, 1H), 7.42 (s, 1H), 7.32 – 7.23 (m, 3H), 4.08 (s, 3H), 3.91 (s, 3H), 3.82 (s, 3H). ^{13}C NMR (101 MHz, $CDCl_3$) δ 176.96, 158.45, 154.89, 152.48, 151.58, 151.33, 149.10, 145.29, 136.23, 129.90, 122.45, 121.68, 121.11, 118.04, 113.53, 108.95, 108.07, 98.71, 58.20, 56.62, 56.42. HRMS (ESI) calcd for $[C_{21}H_{16}BrNO_5 + H]^+$ 442.0290, found 442.02815.

5.2.22. 6,7,10-Trimethoxy-2-(5-methylpyridin-3-yl)-4*H*-benzo[*h*]benzopyran-4-one (**13d**)

Yellow solid; yield 63%; ^{1}H NMR (400 MHz, DMSO-d_6) δ 9.15 (s, 1H), 8.58 (s, 1H), 8.31 (s, 1H), 7.29 –7.11 (m, 4H), 4.02 (s, 3H), 3.91 (s, 3H), 3.83 (s, 3H), 2.43 (s, 3H). ^{13}C NMR (101 MHz, $CDCl_3$) δ 177.20, 160.52, 154.63, 152.21, 151.61, 151.24, 149.13, 144.87, 133.84, 133.23, 127.83, 122.32, 121.57, 118.20, 113.27, 108.94, 107.55, 98.74, 58.13, 56.57, 56.46, 18.55. HRMS (ESI) calcd for $[C_{22}H_{19}NO_5 + H]^+$ 378.1341, found 378.13487.

5.2.23. 2-(5-aminopyridin-3-yl)-6,7,10-trimethoxy-4*H*-benzo[*h*]benzopyran-4-one (**13e**)

Brown solid; yield 54%; ^{1}H NMR (400 MHz, DMSO-d_6) δ 8.49 (s, 1H), 8.17 – 8.02 (m, 1H), 7.54 (s, 1H), 7.26 – 7.08 (m, 3H), 7.01 – 6.87 (m, 1H), 5.61 (s, 2H), 3.98 (s, 3H), 3.87 (s, 3H), 3.78 (s, 3H). ^{13}C NMR (101 MHz, DMSO-d_6) δ 176.14, 161.37, 154.55, 151.12, 151.06, 148.54, 145.21, 139.31, 135.38, 128.03, 121.47, 121.20, 117.73, 116.68, 113.42, 110.17, 107.25, 98.20, 57.72, 57.08, 56.45. HRMS (ESI) calcd for $[C_{21}H_{18}N_2O_5 + H]^+$ 379.1294, found 379.12887.

5.2.24. 5-(6,7,10-trimethoxy-4-oxo-4*H*-benzo[*h*]chroman-2-yl) nicotinic acid (**13f**)

Dark brown solid; yield 39%; ^{1}H NMR (400 MHz, DMSO-d_6) δ 9.57 (s, 1H), 9.21 (d, J = 2.2 Hz, 1H), 9.06 (d, J = 2.7 Hz, 1H), 7.47 (s, 1H), 7.41 – 7.12 (m, 3H), 4.15 (s, 3H), 3.92 (s, 3H), 3.82 (s, 3H). HRMS (ESI) calcd for $[C_{22}H_{17}NO_7 + H]^+$ 408.1083, found 408.14514.

5.2.25. 2-(5-hydroxypyridin-3-yl)-6,7,10-trimethoxy-4*H*-benzo[*h*]benzopyran-4-one (**13g**)

Yellow solid; yield 58%; ^{1}H NMR (400 MHz, DMSO-d_6) δ 8.82 (s, 1H), 8.31 (s, 1H), 7.91 (s, 1H), 7.27 – 7.20 (m, 3H), 7.18 (s, 1H), 4.02 (s, 3H), 3.89 (s, 3H), 3.80 (s, 3H). ^{13}C NMR (101 MHz, DMSO-d_6) δ 176.24, 160.51, 154.68, 154.35, 151.15, 151.11, 148.56, 140.93, 138.51, 128.78, 121.52, 121.27, 119.72, 117.75, 113.56, 110.35, 107.77, 98.21, 57.78, 57.02, 56.53. HRMS (ESI) calcd for $[C_{21}H_{17}NO_6 + H]^+$ 380.1134, found 380.11340.

5.2.26. 2-(6-aminopyridin-3-yl)-6,7,10-trimethoxy-4*H*-benzo[*h*]benzopyran-4-one (**13h**)

Brown solid; yield 48%; ^{1}H NMR (400 MHz, DMSO-d_6) δ 8.84 (d, *J* = 2.3 Hz, 1H), 8.11 (dd, *J* = 8.8, 2.4 Hz, 1H), 7.29 (s, 1H), 7.24 (d, *J* = 2.0 Hz, 2H), 6.93 (s, 1H), 6.78 (s, 2H), 6.57 (d, *J* = 8.8 Hz, 1H), 4.02 (s, 3H), 3.90 (s, 3H), 3.81 (s, 3H). ^{13}C NMR (101 MHz, DMSO-d_6) δ 175.97 , 162.49 , 162.04 , 154.32 , 151.17 , 151.10 , 148.18 , 135.00 , 121.41, 121.10 , 117.87 , 115.58 , 113.18 , 110.16 , 109.99, 108.16 , 103.68 , 98.64 , 57.79 , 57.00 , 56.55. HRMS (ESI) calcd for $[C_{21}H_{18}N_2O_5 + H]^+$ 379.1294, found 379.12959.

5.2.27. 2-(6-hydroxypyridin-3-yl)-6,7,10-trimethoxy-4*H*-benzo[*h*]benzopyran-4-one (**13i**)

Yellow solid; yield 59%; ^{1}H NMR (400 MHz, DMSO-d_6) δ 8.63 (s, 1H), 7.75 (d, *J* = 8.8 Hz, 1H), 7.30 (s, 1H), 7.20 (s, 2H), 6.58 (s, 1H), 5.94 (d, *J* = 9.6 Hz, 1H), 4.01 (s, 3H), 3.89 (s, 3H), 3.80 (s, 3H). HRMS (ESI) calcd for $[C_{21}H_{17}NO_6 + H]^+$ 380.1134, found 380.11406.

5.2.28. 2-(2-hydroxypyridin-3-yl)-6,7,10-trimethoxy-4*H*-benzo[*h*]benzopyran-4-one (**13j**)

Yellow solid; yield 53%; ^{1}H NMR (400 MHz, DMSO-d_6) δ 12.37 (s, 1H), 8.69 (dd, *J* = 7.5, 2.1 Hz, 1H), 7.90 (s, 1H), 7.73 (d, *J* = 6.0 Hz, 1H), 7.37 – 7.17 (m, 3H), 6.64 (t, *J* = 6.8 Hz, 1H), 4.05 (s, 3H), 3.90 (s, 3H), 3.81 (s, 3H). HRMS (ESI) calcd for $[C_{21}H_{17}NO_6 + H]^+$ 380.1134, found 380.11364.

5.2.29. 2-(2-aminopyridin-3-yl)-6,7,10-trimethoxy-4*H*-benzo[*h*]benzopyran-4-one (**13k**)

Brown solid; yield 51%; ^{1}H NMR (400 MHz, DMSO-d_6) δ 12.23 (s, 1H), 10.22 (s, 1H), 8.73 (dd, *J* = 4.4, 1.8 Hz, 1H), 8.45 (dd, *J* = 7.9, 1.8 Hz, 1H), 7.38 (dd, *J* = 7.9, 4.5 Hz, 1H), 7.05 – 6.97 (m, 2H), 6.95 – 6.90 (m, 1H), 6.40 – 6.32 (m, 1H), 3.98 (s, 3H), 3.80 (s, 3H), 3.78 (s, 3H). ^{13}C NMR (101 MHz, DMSO-d_6) δ 177.42, 153.45, 151.52, 151.26, 150.67, 150.41, 149.34, 146.75, 134.76, 120.49, 120.10, 119.53, 117.23, 115.41, 110.92, 109.99, 109.39, 107.39, 57.69, 57.56, 57.36. HRMS (ESI) calcd for $[C_{21}H_{18}N_2O_5 + H]^+$ 379.1294, found 379.13068.

5.2.30. 2-(2-bromopyridin-3-yl)-6,7,10-trimethoxy-4*H*-benzo[*h*]benzopyran-4-one (**13l**)

Yellow solid; yield 56%; ^{1}H NMR (400 MHz, DMSO-d_6) δ 8.71 (d, J = 7.2 Hz, 1H), 7.93 (s, 1H), 7.76 (d, J = 4.6 Hz, 1H), 7.34 – 7.25 (m, 3H), 6.67 (t, J = 6.7 Hz, 1H), 4.08 (s, 3H), 3.93 (s, 3H), 3.85 (s, 3H).

5.2.31. 2-(2-fluoropyridin-4-yl)-6,7,10-trimethoxy-4*H*-benzo[*h*]benzopyran-4-one (**14b**)

Yellow solid; yield 62%; ^{1}H NMR (400 MHz, DMSO-d_6) δ 8.40 (d, J = 5.2 Hz, 1H), 7.74 (d, J = 5.2 Hz, 1H), 7.64 (s, 1H), 7.40 (s, 1H), 7.33 – 7.27 (m, 3H), 4.10 (s, 3H), 3.95 (s, 3H), 3.85 (s, 3H). ^{13}C NMR (101 MHz, $CDCl_3$) δ 177.34, 164.85, 159.93, 154.70, 151.65, 151.19, 149.04, 147.62, 142.14, 122.42, 121.68, 118.13, 113.37, 112.43, 108.94, 108.42, 108.31, 98.58, 58.10, 56.54, 56.36.

5.2.32. 2-(2-chloropyridin-4-yl)-6,7,10-trimethoxy-4*H*-benzo[*h*]benzopyran-4-one (**14c**)

Yellow solid; yield 61%; ^{1}H NMR (400 MHz, DMSO-d_6) δ 8.71 (d, J = 5.1 Hz, 1H), 8.35 (s, 1H), 8.22 (d, J = 5.1 Hz, 1H), 7.55 (s, 1H), 7.36 – 7.34 (m, 2H), 7.32 (s, 1H), 4.15 (s, 3H), 3.96 (s, 3H), 3.86 (s, 3H). HRMS (ESI) calcd for $[C_{21}H_{16}ClNO_5 + H]^+$ 398.0795, found 398.0793.

5.2.33. 2-(2-Bromo-pyridin-4-yl)-6,7,10-trimethoxy-4*H*-benzo[*h*]benzopyran-4-one (**14d**)

Yellow solid; yield 65%; ^{1}H NMR (400 MHz, $CDCl_3$) δ 8.55 (d, J = 5.3 Hz, 1H), 8.41 (s, 1H), 7.76 (d, J = 5.4 Hz, 1H), 7.49 (d, J = 10.2 Hz, 1H), 7.17 (d, J = 8.6 Hz, 1H), 7.11 (d, J = 8.5 Hz, 1H), 7.05 (s, 1H), 4.18 (s, 3H), 4.07 (s, 3H), 3.95 (s, 3H). ^{13}C NMR (101 MHz, $CDCl_3$) δ 177.06, 158.10, 155.06, 151.61, 151.32, 150.76, 149.05, 143.45, 142.21, 129.69, 124.82, 122.53, 121.86, 118.38, 117.92, 113.64, 109.06, 98.49, 58.17, 56.62, 56.47.

5.2.34. 2-(2-hydroxypyridin-4-yl)-6,7,10-trimethoxy-4*H*-benzo[*h*]benzopyran-4-one (**14e**)

Yellow solid; yield 66%; ^{1}H NMR (400 MHz, DMSO-d_6) δ 11.91 (s, 1H), 7.59 (d, J = 6.8 Hz, 1H), 7.38 – 7.26 (m, 5H), 6.92 (d, J = 6.8 Hz, 1H), 4.09 (s, 3H), 3.95 (s, 1H), 3.86 (s, 1H). HRMS (ESI) calcd for $[C_{21}H_{17}NO_6 + H]^+$ 380.1134, found 380.11428.

5.2.35. 2-(2-aminopyridin-4-yl)-6,7,10-trimethoxy-4*H*-benzo[*h*]benzopyran-4-one (**14f**)

Brown solid; yield 54%; ^{1}H NMR (400 MHz, DMSO-d_6) δ 8.15 (s, 1H), 7.32 (s, 3H), 7.24 (s, 1H), 7.18 (s, 1H), 7.11 (s, 1H), 6.24 (s, 2H), 4.09 (s, 3H), 3.95 (s, 3H), 3.85 (s, 3H). ^{13}C NMR (101 MHz, $CDCl_3$) δ 177.43, 160.49, 159.01, 154.77, 151.65, 151.41, 149.11, 148.46, 141.74, 122.45, 121.76, 118.36, 113.39, 110.28, 109.55, 108.53, 105.29, 98.66, 58.15, 56.80, 56.60. HRMS (ESI) calcd for $[C_{21}H_{18}N_2O_5 + H]^+$ 379.1294, found 379.12943.

622

623 5.2.36. 2-(3-aminopyridin-4-yl)-6,7,10-trimethoxy-4*H*-benzo[*h*]benzopyran-4-one (**14g**)

624 Brown solid; yield 59%; ^{1}H NMR (400 MHz, DMSO-d_6) δ 9.08 (s, 1H), 8.41 (d, J = 5.0 Hz, 1H),
625 7.89 (d, J = 4.9 Hz, 1H), 7.11 – 6.98 (m, 2H), 6.98 – 6.91 (m, 1H), 6.48 (s, 1H), 3.98 (s, 3H), 3.82
626 (d, J = 13.4 Hz, 3H), 3.79 (s, 3H). HRMS (ESI) calcd for $[C_{21}H_{18}N_2O_5 + H]^+$ 379.1294, found
627 379.12930. HRMS (ESI) calcd for $[C_{21}H_{18}N_2O_5 + H]^+$ 379.1294, found 379.12930.

628

629 5.2.37. 2-(6-aminopyridin-2-yl)-6,7,10-trimethoxy-4*H*-benzo[*h*]benzopyran-4-one (**15b**)

630 Brown solid; yield 55%; ^{1}H NMR (400 MHz, DMSO-d_6) δ 7.76 – 7.64 (m, 1H), 7.57 (d, J = 7.5
631 Hz, 1H), 7.27 (s, 1H), 7.25 (s, 2H), 7.16 (s, 1H), 6.65 (d, J = 7.9 Hz, 1H), 6.29 (s, 2H), 4.05 (s,
632 3H), 3.90 (s, 3H), 3.81 (s, 3H). ^{13}C NMR (101 MHz, $CDCl_3$) δ 177.95, 161.84, 158.04, 154.34,
633 151.78, 151.30, 148.40, 138.27, 122.37, 122.03, 118.51, 117.98, 113.83, 113.07, 111.80, 110.99,
634 109.18, 99.15, 58.20, 56.79, 56.60. HRMS (ESI) calcd for $[C_{21}H_{18}N_2O_5 + H]^+$ 379.1294, found
635 379.12958.

636

637 5.2.38. 2-(6-hydroxypyridin-2-yl)-6,7,10-trimethoxy-4*H*-benzo[*h*]benzopyran-4-one (**15c**)

638 Yellow solid; yield 61%; ^{1}H NMR (400 MHz, DMSO-d_6) δ 11.00 (s, 1H), 7.80 (s, 1H), 7.53 (s,
639 1H), 7.34 – 6.96 (m, 4H), 6.72 (d, J = 7.9 Hz, 1H), 4.00 (s, 3H), 3.85 (s, 3H), 3.77 (s, 3H). HRMS
640 (ESI) calcd for $[C_{21}H_{17}NO_6 + H]^+$ 380.1134, found 380.11321.

641

642 5.2.39. 6,7,10-Trimethoxy-2-(6-methylpyridin-2-yl)-4*H*-benzo[*h*]benzopyran-4-one (**15d**)

643 Yellow solid; yield 64%; ^{1}H NMR (400 MHz, DMSO-d_6) δ 8.19 (d, J = 7.7 Hz, 1H), 8.07 (t, J =
644 7.8 Hz, 1H), 7.49 (d, J = 7.8 Hz, 1H), 7.36 – 7.26 (m, 4H), 4.12 (s, 3H), 3.94 (s, 3H), 3.85 (s, 3H),
645 2.60 (s, 3H). ^{13}C NMR (101 MHz, $CDCl_3$) δ 177.76, 161.57, 158.68, 154.32, 151.49, 151.14,
646 149.17, 148.75, 136.74, 124.85, 122.16, 121.91, 118.19, 118.06, 112.89, 108.89, 107.88, 98.90,
647 58.00, 56.52, 56.46, 24.53. HRMS (ESI) calcd for $[C_{22}H_{19}NO_5 + H]^+$ 378.1341, found 378.13490.

648

649 5.2.40. 2-(6-fluoropyridin-2-yl)-6,7,10 trimethoxy-4*H*-benzo[*h*]benzopyran-4-one (**15e**)

650 Yellow solid; yield 60%; ^{1}H NMR (400 MHz, DMSO-d_6) δ 8.43 (d, J = 7.7 Hz, 1H), 8.32 – 8.25
651 (m, 1H), 7.48 (d, J = 7.6 Hz, 1H), 7.36 – 7.24 (m, 3H), 7.17 (s, 1H), 4.14 (s, 3H), 3.95 (s, 3H),
652 3.86 (s, 3H). ^{13}C NMR (101 MHz, $CDCl_3$) δ 177.47, 164.07, 161.67, 159.47, 154.57, 151.39,
653 151.24, 148.64, 141.82, 122.20, 121.96, 118.32, 118.03, 113.03, 111.78, 111.41, 109.06, 98.75,
654 57.96, 56.56, 56.46. HRMS (ESI) calcd for $[C_{21}H_{16}FNO_5 + H]^+$ 382.1091, found 382.10968.

655

5.2.41. 2-(6-chloropyridin-2-yl)-6,7,10-trimethoxy-4*H*-benzo[*h*]benzopyran-4-one (**15f**)
Yellow solid; yield 56%; ^{1}H NMR (400 MHz, DMSO-d_6) δ 8.26 (d, J = 7.0 Hz, 2H), 7.74 (d, J = 7.0 Hz, 1H), 7.27 (s, 3H), 7.16 (s, 1H), 4.09 (s, 3H), 3.91 (s, 1H), 3.82 (s, 1H). ^{13}C NMR (101 MHz, $CDCl_3$) δ 177.45, 159.53, 154.61, 151.53, 151.44, 151.29, 150.49, 148.69, 139.28, 125.87, 122.04, 119.34, 118.11, 113.11, 109.96, 109.13, 108.73, 98.79, 58.05, 56.64, 56.50. HRMS (ESI) calcd for $[C_{21}H_{16}ClNO_5 + H]^+$ 398.0795, found 398.08009.

5.2.42. 2-(5-chloropyridin-2-yl)-6,7,10-trimethoxy-4*H*-benzo[*h*]benzopyran-4-one (**15g**)
Yellow solid; yield 57%; ^{1}H NMR (400 MHz, DMSO-d_6) δ 8.86 (s, 1H), 8.42 – 8.30 (m, 2H), 7.34 – 7.20 (m, 4H), 4.11 (s, 3H), 3.92 (s, 1H), 3.82 (s, 1H).

5.2.43. 2-(4-chloropyridin-2-yl)-6,7,10-trimethoxy-4*H*-benzo[*h*]benzopyran-4-one (**15h**)
Yellow solid; yield 49%; ^{1}H NMR (400 MHz, DMSO-d_6) δ 8.77 (s, 1H), 8.41 (s, 1H), 7.81 (s, 1H), 7.30 (m, 4H), 4.13 (s, 3H), 3.95 (s, 3H), 3.86 (s, 3H). HRMS (ESI) calcd for $[C_{21}H_{16}ClNO_5 + H]^+$ 398.0795, found 398.07919.

5.2.44. 2-(5-fluoropyridin-2-yl)-6,7,10 trimethoxy-4*H*-benzo[*h*]benzopyran-4-one (**15i**)
Yellow solid; yield 56%; ^{1}H NMR (400 MHz, $CDCl_3$) δ 8.53 (s, 1H), 8.43 – 8.35 (m, 1H), 7.54 (s, 2H), 7.47 (s, 1H), 7.10 (d, J = 9.0 Hz, 1H), 7.04 (d, J = 8.9 Hz, 1H), 4.05 (s, 3H), 4.01 (s, 3H), 3.89 (s, 3H). ^{13}C NMR (101 MHz, $CDCl_3$) δ 177.62, 161.53, 160.41, 158.93, 154.62, 151.58, 151.49, 148.70, 146.38, 138.73, 138.48, 123.37, 123.19, 122.40, 122.03, 118.37, 113.21, 109.37, 108.14, 99.10, 58.20, 56.84, 56.60. HRMS (ESI) calcd for $[C_{21}H_{16}FNO_5 + H]^+$ 382.1091, found 382.10886.

5.2.45. 2-(5-Bromopyridin-2-yl)-6,7,10-trimethoxy-4*H*-benzo[*h*]benzopyran-4-one (**15j**)
Yellow solid; yield 53%; ^{1}H NMR (400 MHz, DMSO-d_6) δ 8.83 (s, 1H), 8.42 (s, 1H), 8.14 (s, 1H), 7.28 – 7.17 (m, 4H), 4.03 (s, 3H), 3.88 (s, 3H), 3.80 (s, 3H). ^{13}C NMR (101 MHz, $CDCl_3$) δ 177.47, 160.19, 154.53, 151.27, 150.87, 149.77, 148.54, 148.38, 139.28, 136.71, 122.59, 122.00, 121.03, 117.97, 112.87, 108.98, 108.10, 98.69, 57.93, 56.52, 56.47. HRMS (ESI) calcd for $[C_{21}H_{16}BrNO_5 + H]^+$ 442.0290, found 442.02948.

5.2.46. 2-(5-aminopyridin-2-yl)-6,7,10-trimethoxy-4*H*-benzo[*h*]benzopyran-4-one (**15k**)
Brown solid; yield 50%; ^{1}H NMR (400 MHz, DMSO-d_6) δ 8.14 – 8.00 (m, 2H), 7.30 (s, 1H), 7.28 – 7.22 (m, 2H), 7.16 – 7.10 (m, 1H), 7.02 (s, 1H), 6.19 (brs, 2H), 4.07 (s, 3H), 3.91 (s, 3H),

3.82 (s, 3H). ^{13}C NMR (101 MHz, DMSO-d_6) δ 176.02, 162.89, 154.43, 151.19, 148.06, 147.77, 137.22, 135.97, 122.65, 121.52, 121.49, 119.31, 117.90, 113.21, 110.27, 104.03, 98.73, 57.85, 57.20, 56.59. HRMS (ESI) calcd for $[C_{21}H_{18}N_2O_5 + H]^+$ 379.1294, found 379.12981.

5.3. CYP1 enzyme inhibition assay

The inhibitory activity of these synthesized compounds against recombinant human CYP1 enzymes was measured by EROD (7-ethoxyresorufin O-deethylase) assay according to our previously reported procedure[17, 18]. The recombinant human CYP1 enzymes including CYP1B1, CYP1A1, and CYP1A2, each equipped with P450 reductase (Supersomes), were obtained from BD Genetest (Corning). Substrate 7-Ethoxyresorufin (7-ER) and $MgCl_2$ were purchased from Sigma-Aldrich. D-glucose-6-phosphate (G-6-P), glucose-6-phosphate dehydrogenase (G-6-PD) and nicotinamide-adenine dinucleotide phosphate ($NADP^+$) were purchased from Biosharp Co., Ltd. In brief, a mixture with a final volume of 200 μl containing various concentrations of tested compounds (except positive and negative control wells), an enzyme source (20 fmol CYP1B1, 10 fmol CYP1A1 or 60 fmol CYP1A2), substrate (7-ER, 150 nM) and a NADPH regeneration system (1.3 mM $NADP^+$, 3.3 mM G-6-P, 0.5 U/mL G-6-PD and 3.3 mM $MgCl_2$) was incubated in a black 96-well flat-bottomed microplate at 37 ^oC for varied time durations (CYP1B1 35 min; CYP1A1 15 min; CYP1A2 50 min). Then, the reaction was quenched by addition of 100 μl of pre-cooled methanol to all wells, and the fluorescence intensity was determined by FlexStation 3 apparatus with excitation and emission filters at 544 and 590 nm, respectively. Three replicates were used for each concentration. The IC_{50} values were calculated from the non-linear regression formula, log (inhibitor) *vs*. normalized response-variable slope, by the GraphPad Prism Software (Version 5.0).

5.4 Molecular docking procedure

The X-ray structure coordinates of ANF bound with CYP1B1 (PDB entry 3PM0) or CYP1A2 (PDB entry 2HI4) were achieved from RCSB protein data bank (http://www.rcsb.org/). The modelling experiments described in this study were performed by the docking programs of GOLD 5.3.0 and SYBYL-X 2.0. All water molecules in the crystal structure of CYP1B1 were removed prior to docking, but water molecules in the crystal structure of CYP1A2 were retained for docking study owing to its possible role in formation of water-mediated hydrogen bond. For docking with GOLD 5.3.0, the ligands were drawn in ChemBio 3D Ultra software (2014) and subjected to energy minimization using the MM2 force field. The docking protocol was validated by reproducing the pose of ANF at the binding site in CYP1B1 or CYP1A2. For docking with

SYBYL-X 2.0, ligands were constructed with Sybyl/Sketch module and optimized applying Powell's method with Tripos force field with convergence criterion set at 0.05 kcal/(Å mol), and assigned with Gasteiger-Hückel method. Hydrogen and missing atoms of the protein were added and the co-crystallized ligand (ANF) served as a template to generate protomol with a threshold of 0.50 as default setting. Docking calculations were carried out with Surflex-Dock with other docking parameters as default.

5.5 Determination of water-solubility

A high-performance liquid chromatographic (HPLC) method (Eclipse plus C18, 3.5 μm, 4.6×100 mm (Agilent)) was used to determine their water solubilities. Briefly, Standard stock solutions were prepared by dissolving 5 mg of each compound in 1 mL of the mixture solvent of DCM and MeOH. Then, the stock solution was diluted by MeOH to yield concentrations of 2000, 1500, 1000, 500, 350, 250 and 125 μg/mL or 5000, 4000, 3000, 2000,1500, 1000 and 500 μg/mL (for the salt form of compound **13h**) were injected into HPLC (by dilution if necessary) and detected at wavelength of 360 nm. Next, a volume of 10 μL supersaturated solution of the compounds (by dilution if necessary) in water were injected into HPLC for analysis (detection wavelength at 360 nm). The water solubility was calculated according to the linear regression equation.

Declaration of competing interest

The authors declare no conflicts of interest.

Acknowledgements

This program was supported by National Natural Science Foundation of China (Grant No. 21602132 and No. 81673281), the Interdisciplinary Program of Shanghai Jiao Tong University (project number: ZH2018QNB15) and Zhejiang Chinese Medical University Startup Funding (2020ZR12). We also want to express our gratitude to associate professor Xiaoyan Pan and professor Jie Zhang in the Xi'an Jiaotong University for providing molecular docking software.

Reference

[1] D. Lang, M. Radtke, M. Bairlein, Highly Variable Expression of CYP1A1 in Human Liver and Impact on Pharmacokinetics of Riociguat and Granisetron in Humans, Chem. Res. Toxicol. 32 (2019) 1115-1122.

[2] J. Dong, Q. Zhang, Q. Cui, G. Huang, X. Pan, S. Li, Flavonoids and Naphthoflavonoids:

Wider Roles in the Modulation of Cytochrome P450 Family 1 Enzymes, ChemMedChem 11 (2016) 2102-2118.

[3] C. A. Piccinato, R. M. Neme, N. Torres, L. R. Sanches, P. B. M. Cruz Derogis, H. F. Brudniewski, J. C. R. E Silva, R.A. Ferriani, Increased expression of CYP1A1 and CYP1B1 in ovarian/peritoneal endometriotic lesions, Reproduction 151 (2016) 683-692.

[4] R. Dutour, D. Poirier, Inhibitors of cytochrome P450 (CYP) 1B1, Eur. J. Med. Chem. 135 (2017) 296-306.

[5] H. Takemura, H. Nagayoshi, T. Matsuda, H. Sakakibara, M. Morita, A. Matsui, T. Ohura, K. Shimoi, Inhibitory effects of chrysoeriol on DNA adduct formation with benzo[a]pyrene in MCF-7 breast cancer cells, Toxicology 274 (2010) 42-48.

[6] S. Kim, H. Ko, J. E. Park, S. Jung, S. K. Lee, Y. J. Chun, Design, Synthesis, and Discovery of Novel trans-Stilbene Analogues as Potent and Selective Human Cytochrome P450 1B1 Inhibitors, J. Med. Chem. 45 (2002) 160-164.

[7] K. Endo, S. Uno, T. Seki, T. Ariga, Y. Kusumi, M. Mitsumata, S. Yamada, M. Makishima, Inhibition of aryl hydrocarbon receptor transactivation and DNA adduct formation by CYP1 isoform-selective metabolic deactivation of benzo[a]pyrene, Toxicol. Appl. Pharmacol. 230 (2008) 135-143.

[8] R. Dutour, F. Cortés-Benítez, J. Roy, D. Poirier, Structure-Based Design and Synthesis of New Estrane–Pyridine Derivatives as Cytochrome P450 (CYP) 1B1 Inhibitors, ACS Med. Chem. Lett. 8 (2017) 1159-1164.

[9] M. C. E. McFadyen, G. I. Murray, Cytochrome P450 1B1: a novel anticancer therapeutic target, Future Oncol. 1 (2005) 259-263.

[10] M. U. Mohd Siddique, T. K. Barbhuiya, B. N. Sinha, V. Jayaprakash, Phytoestrogens and their synthetic analogues as substrate mimic inhibitors of CYP1B1, Eur. J. Med. Chem. 163 (2019) 28-36.

[11] J. Dong, G. Huang, Q. Zhang, Z. Wang, J. Cui, Y. Wu, Q. Meng, S. Li, Development of benzochalcone derivatives as selective CYP1B1 inhibitors and anticancer agents, MedChemComm 10 (2019) 1606-1614.

[12] J. Dong, Z. Qin, W. D. Zhang, G. Cheng, A. G. Yehuda, C. R. Ashby, Z. S. Chen, X. D. Cheng, J. J. Qin, Medicinal chemistry strategies to discover P-glycoprotein inhibitors: An update, Drug Resist. Updates 49 (2020) 100681.

[13] J. Dong, Q. Zhang, Q. Meng, Z. Wang, S. Li, J. Cui, The Chemistry and Biological Effects of Thioflavones, Mini. Rev. Med. Chem. 18 (2018) 1714-1732.

[14] T. Shimada, H. Yamazaki, M. Foroozesh, N. E. Hopkins, W. L. Alworth, F. P. Guengerich,

Selectivity of Polycyclic Inhibitors for Human Cytochrome P450s 1A1, 1A2, and 1B1, Chem. Res. Toxicol. 11 (1998) 1048-1056.

[15] M. C. E. McFadyen, H. L. McLeod, F. C. Jackson, W. T. Melvin, J. Doehmer, G. I. Murray, Cytochrome P450 CYP1B1 protein expression: A novel mechanism of anticancer drug resistance11Abbreviations: CYP, cytochrome P450; ANF, alpha-naphthoflavone; MTT, 3-[4,5-dimethylthiazol-2yl]-2,5-diphenyltetrazolium bromide; and 5-FU, 5-fluorouracil, Biochem. Pharmacol. 62 (2001) 207-212.

[16] A. Datta, N. Bhasin, H. Kim, M. Ranjan, B. Rider, Z. Y. Abd Elmageed, D. Mondal, K. C. Agrawal, A. B. Abdel-Mageed, Selective targeting of FAK-Pyk2 axis by alpha-naphthoflavone abrogates doxorubicin resistance in breast cancer cells, Cancer Lett. 362 (2015) 25-35.

[17] J. Cui, Q. Meng, X. Zhang, Q. Cui, W. Zhou, S. Li, Design and Synthesis of New α-Naphthoflavones as Cytochrome P450 (CYP) 1B1 Inhibitors To Overcome Docetaxel-Resistance Associated with CYP1B1 Overexpression, J. Med. Chem. 58 (2015) 3534-3547.

[18] J. Dong, Z. Wang, J. Cui, Q. Meng, S. Li, Synthesis and structure-activity relationship studies of α-naphthoflavone derivatives as CYP1B1 inhibitors, Eur. J. Med. Chem. 187 (2020) 111938.

[19] J. Dong, Z. Wang, Q. Meng, Q. Zhang, G. Huang, J. Cui, S. Li, Development of 2-arylbenzo [*h*] quinolone analogs as selective CYP1B1 inhibitors, RSC Adv. 8 (2018) 15009-15020.

[20] S. Sansen, J. K. Yano, R. L. Reynald, G. A. Schoch, K. J. Griffin, C. D. Stout, E. F. Johnson, Adaptations for the oxidation of polycyclic aromatic hydrocarbons exhibited by the structure of human P450 1A2, J. Biol. Chem. 282 (2007) 14348-14355.

[21] A. Wang, U. Savas, C. D. Stout, E. F. Johnson, Structural characterization of the complex between alpha-naphthoflavone and human cytochrome P450 1B1, J. Biol. Chem. 286 (2011) 5736-5743.

[22] B. Lin, J. H. Pease, A high throughput solubility assay for drug discovery using microscale shake-flask and rapid UHPLC-UV-CLND quantification, J. Pharm. Biomed. Anal. 122 (2016) 126-140.

[23] J. H. Cui, W. Zhou, S. S. Li, A Convenient and Efficient Synthesis of 2-Acetyl-5,8-Dimethoxy-1,4-Naphthoquinone, J. Chem. Res. 36 (2012) 264-265.

Table 1. Inhibitory activities of 6,7,10-trimethoxy-α-naphthoflavone derivatives against CYP1s

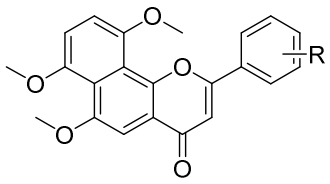

Compd.	R	IC_{50} values (nM)			IC_{50} ratio	
		1B1	1A1	1A2	1A1/1B1	1A2/1B1
11a	3-(4-methyl-piperazin-1-yl)	>1000	>1000	>1000	-	-
11b	3-Cl-5-(4-methyl-piperazin-1-yl)	519.4	>1000	>1000	>1.9	>1.9
11c	3-(4-morpholinyl)	14.9	132.5	>1000	8.9	>67.1
11d	4-(4-methyl-piperazin-1-yl)	>1000	>1000	>1000	-	-
ANF	-	5.9	80.3	18.0	13.6	3.1

Table 2. Inhibitory activities of heterocyclic ring-substituted

6,7,10-trimethoxy-α-naphthoflavone derivatives toward CYP1 enzymes

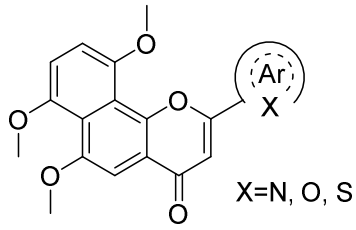

Compd.	Ar	IC_{50} values (nM)			IC_{50} ratio	
		1B1	1A1	1A2	1A1/1B1	1A2/1B1
12a	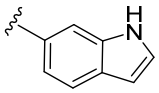	0.95	141.9	>1000	149.4	>1052.6
12b	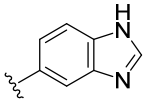	15.6	42.4	>1000	2.7	>64.1
12c	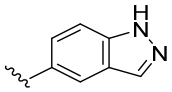	2.0	1.6	>1000	0.8	>500
12d	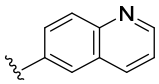	1.8	20.9	>1000	11.6	>555.6
12e	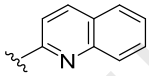	1.0	117.6	>1000	117.6	>1000
12f	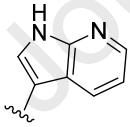	189.4	23.8	>1000	0.1	>5.3
12g	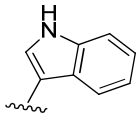	4.1	16.5	>1000	4.0	>243.9
12h	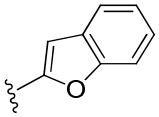	0.87	10.1	>1000	11.6	>1149.4
12i	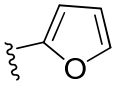	1.2	13.8	67.2	11.5	56.0
12j	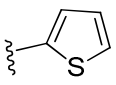	4.8	4.4	40.4	0.9	8.4

Compd.	Ar	IC_{50} values (nM)			IC_{50} ratio	
		1B1	1A1	1A2	1A1/1B1	1A2/1B1
12k	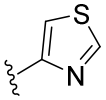	2.6	3.1	29.2	1.2	11.2
12l	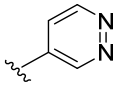	2.0	125.7	>1000	62.9	>500
13a	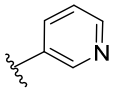	1.0	7.6	117.3	7.6	117.3
14a	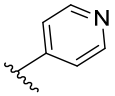	1.2	40.4	199.8	33.7	166.5
15a	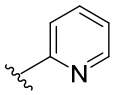	0.6	5.4	107.6	9.0	179.3
ANF	-	5.9	80.3	18.0	13.6	3.1

Table 3. Inhibitory activities of pyridin-3-yl substituted 6,7,10-trimethoxy-α-naphthoflavone derivatives toward CYP1s

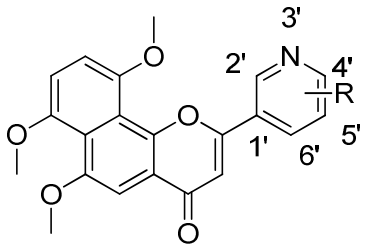

Compd.	R	IC_{50} values (nM)			IC_{50} ratio	
		1B1	1A1	1A2	1A1/1B1	1A2/1B1
13a	H	1.0	7.6	117.3	7.6	117.3
13b	5’-F	0.98	17.7	140.6	18.1	143.5
13c	5’-Br	1.1	8.0	742.0	7.3	674.5
13d	5’-CH_3	1.3	6.9	160.7	5.3	123.6
13e	5’-NH_2	22.9	18.8	628.5	0.8	27.4
13f	5’-COOH	30.1	85.8	>1000	2.9	>33.2
13g	5’-OH	10.3	80.9	>1000	7.9	>97.1
13h	4’-NH_2	0.98	30.8	108.0	31.4	110.2
13i	4’-OH	658.3	>1000	>1000	>1.5	>1.5
13j	2’-OH	>1000	151.9	>1000	0.2	-
13k	2’-NH_2	175.2	137.1	>1000	0.8	>5.7
13l	2’-Br	63.9	60.7	965.5	0.9	15.1
ANF	-	5.9	80.3	18.0	13.6	3.1

Table 4. Inhibitory activities of pyridin-4-yl substituted 6,7,10-trimethoxy-α-naphthoflavone derivatives toward CYP1s

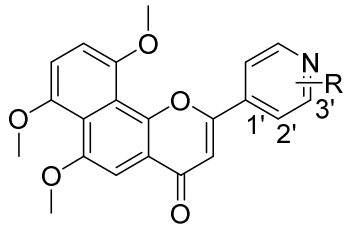

Compd.	R	IC_{50} values (nM)			IC_{50} ratio	
		1B1	1A1	1A2	1A1/1B1	1A2/1B1
14a	H	1.2	40.4	199.8	33.7	166.5
14b	3'-F	0.93	38.9	518.0	41.8	557.0
14c	3'-Cl	1.1	91.6	>1000	83.3	>909.1
14d	3'-Br	0.46	26.9	>1000	58.5	>2173.9
14e	3'-OH	61.5	232.0	>1000	3.8	>16.3
14f	3'-NH_2	20.6	15.3	>1000	0.7	>48.5
14g	2'-NH_2	24.8	31.6	>1000	1.3	>40.3
ANF	-	5.9	80.3	18.0	13.6	3.1

Table 5. Inhibitory activities of pyridin-2-yl substituted 6,7,10-trimethoxy-α-naphthoflavone derivatives toward CYP1s

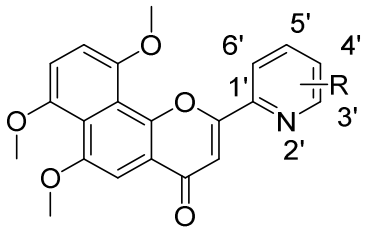

Compd.	R	IC_{50} values (nM)			IC_{50} ratio	
		1B1	1A1	1A2	1A1/1B1	1A2/1B1
ANF	-	5.9	80.3	18.0	13.6	3.1
15a	H	0.6	5.4	107.6	9.0	179.3
15b	3’-NH_2	6.5	56.8	>1000	8.7	>153.8
15c	3’-OH	7.7	322.6	>1000	41.9	>129.9
15d	3’-CH_3	1.2	19.9	148.2	16.6	123.5
15e	3’-F	0.38	2.3	668.4	6.1	1758.9
15f	3’-Cl	0.30	5.7	348.6	19.0	1162
15g	4’-Cl	0.14	1.6	208.5	11.4	1489.3
15h	5’-Cl	0.84	9.9	>1000	11.8	>1190.5
15i	4’-F	0.07	16.8	>1000	240	>14285.7
15j	4’-Br	1.3	38.9	622.8	29.9	479.1
15k	4’-NH_2	6.0	66.6	>1000	11.1	>166.7

Table 6. Surflex-Dock scores of compound **15i** and ANF

Compd.	IC_{50} values (nM)		Docking score in CYP1B1			Docking score in CYP1A2		
	CYP1B1	CYP1A2	Total Score	Crash Score	Polar Score	Total Score	Crash Score	Polar Score
15i	0.07	>1000	8.5969	-2.5712	0.0001	4.1880	-7.4502	1.1228
ANF	5.9	18.0	6.9699	-0.3755	0.0000	7.1981	-0.3857	0.1418

(Total score, expressed as -log(K_d), represent binding affinities; Crash score, degree of inappropriate penetration by the ligand into the protein and interpenetration between ligand atoms that are separated by rotatable bonds of compounds. c) Polar score, the contribution of polar non-hydrogen bonding interactions to the total score)

Table 7. Water solubility of the selected compounds.

Compd.	ClogP	Water solubility (μg/mL)	
		Free base	Salt form
ANF	4.65	< 5	/
15i	3.75	< 5	< 5
13h	2.99	311	4910

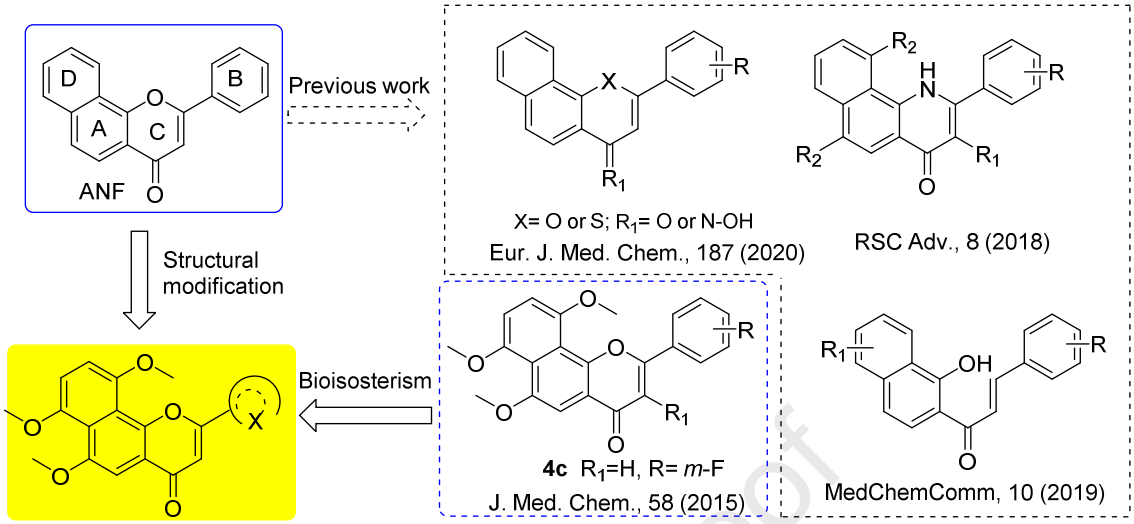

Fig 1. Summary of our previous and current work.

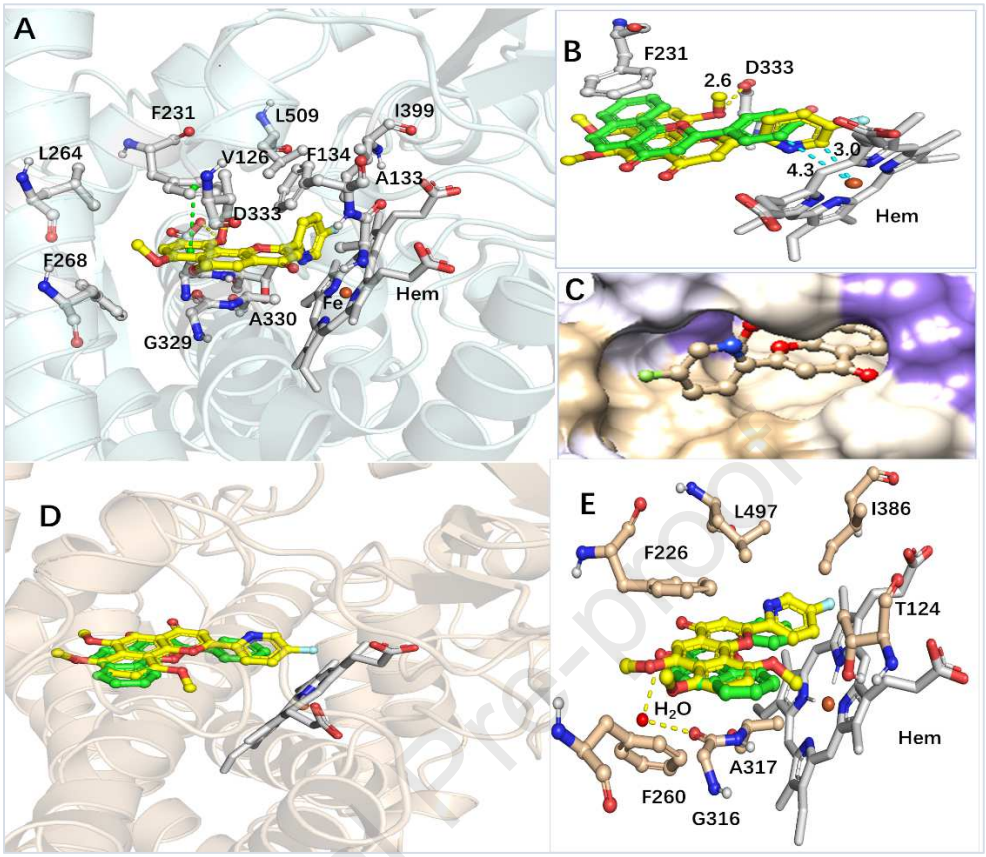

Fig 2. Molecular docking study of compound **15i** in CYP1B1(A-C) and CYP1A2 (D-E) (compound **15i**: yellow stick; ANF: green stick; yellow dash line: hydrogen bond; green dash line: π-π stacking interaction; cyan dash line: distance)

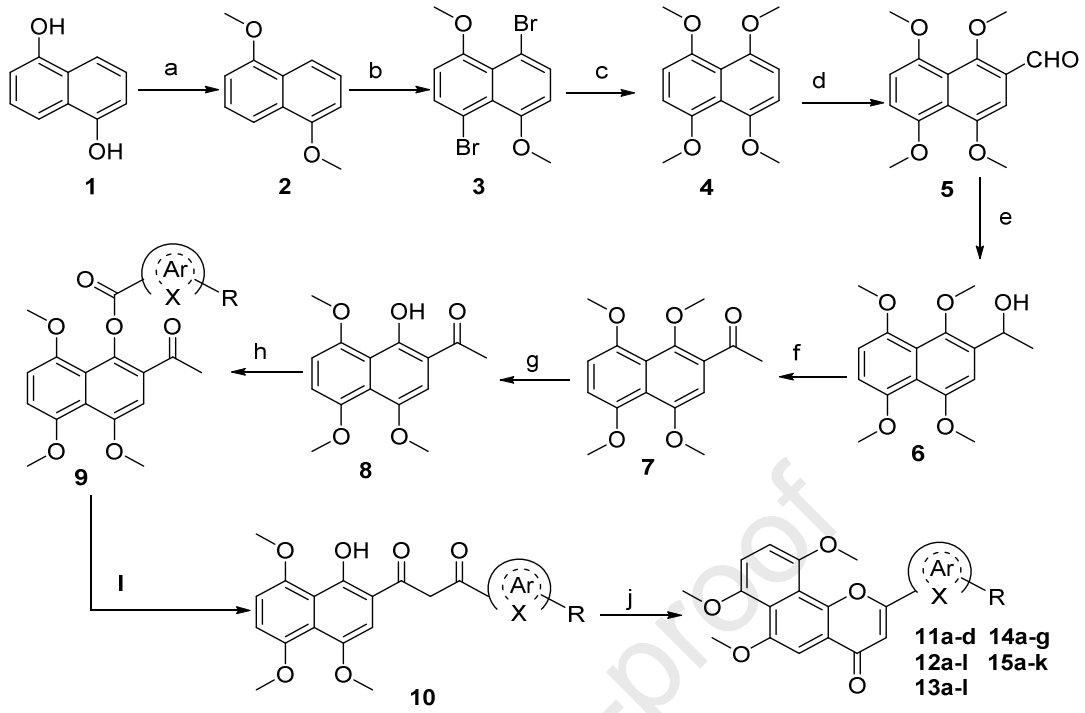

Scheme 1. Reagents and conditions: (a) KOH, $(CH_3)_2SO_4$, rt.; (b) CH_3CN, NBS, -10 ^oC; (c) CH_3ONa, CuI, reflux; (d) $POCl_3$, DMF, reflux; (e) CH_3MgI, Et_2O, NH_4Cl, rt.; (f) MnO_2, DCM, reflux; (g) $AlCl_3$, CH_3CN, 60 ^oC; (h) EDCI/DMAP or HATU/DMAP; (i) NaH, DMF; (j) 10% H_2SO_4-EtOH, reflux.

Highlights

- Discovery of some potent CYP1B1 inhibitors with high selectivity
- Expanding the structure-activity relationship of α-naphthoflavone derivatives as CYP1 inhibitors
- Discovery of a potent and selective CYP1B1 inhibitor with improved water-solubility

Declaration of competing interest

The authors declare no conflicts of interest.